

Weierstraß-Institut
für Angewandte Analysis und Stochastik
Leibniz-Institut im Forschungsverbund Berlin e. V.

Preprint

ISSN 2198-5855

**A kinetic equation for the distribution of interaction clusters in
rarefied gases**

Robert I. A. Patterson¹, Sergio Simonella², Wolfgang Wagner¹

submitted: January 12, 2017

¹ Weierstrass Institute
Mohrenstr. 39
10117 Berlin, Germany
E-Mail: robert.patterson@wias-berlin.de
wolfgang.wagner@wias-berlin.de

² Zentrum Mathematik, TU München
Boltzmannstr. 3
85748 Garching, Germany
E-Mail: s.simonella@tum.de

No. 2365
Berlin 2017



2010 *Mathematics Subject Classification.* 60K35, 82B40.

Key words and phrases. Stochastic particle system, interaction clusters, rarefied gases, kinetic equation, numerical experiments.

Edited by
Weierstraß-Institut für Angewandte Analysis und Stochastik (WIAS)
Leibniz-Institut im Forschungsverbund Berlin e. V.
Mohrenstraße 39
10117 Berlin
Germany

Fax: +49 30 20372-303
E-Mail: preprint@wias-berlin.de
World Wide Web: <http://www.wias-berlin.de/>

Abstract

We consider a stochastic particle model governed by an arbitrary binary interaction kernel. A kinetic equation for the distribution of interaction clusters is established. Under some additional assumptions a recursive representation of the solution is found. For particular choices of the interaction kernel (including the Boltzmann case) several explicit formulas are obtained. These formulas are confirmed by numerical experiments. The experiments are also used to illustrate various conjectures and open problems.

Contents

1 Introduction	2
2 Stochastic model	3
3 Kinetic equation	4
3.1 Derivation of the equation	4
3.2 General properties	6
3.2.1 Total velocity distribution	9
3.2.2 Velocity distributions in the clusters	10
3.2.3 Cluster size distribution	11
3.2.4 Gelation time	12
3.3 Specifications	14
3.3.1 Invertible collision transformations	14
3.3.2 Invariance condition	15
3.3.3 Constant interaction rates	17
3.3.4 Multi-colour clusters	21
4 Boltzmann interactions	23
4.1 Hard sphere gas	26
4.2 Special collision kernel	28
4.3 Numerical experiments	34
4.3.1 Cluster properties	35
4.3.2 Gelation time	40
4.3.3 Billiard model	42
5 Comments	45
References	46

1 Introduction

Interaction clusters provide the decomposition of a particle system with localized interactions into groups of particles that have influenced each other up to a given time. The evolution of interaction clusters in a frictionless elastic billiard model was studied in [6]. Based on numerical experiments, a phase transition in the cluster formation process was observed. Namely, at some critical time a sharp qualitative change occurs: “There appears a distinctive largest cluster, which creates a gap in the mass distribution between the largest cluster and the rest of the clusters.” Further results on this issue were obtained in [11]. The dynamics of interaction clusters was put into the context of rare event simulations in [5], where the application areas range from earthquake prediction to socio-economic phenomena. In order to understand the mechanism of the phase transition it is helpful to study various characteristics of the cluster formation process, such as the distribution of the size of the clusters and the statistics of particles in a cluster.

The paper [6] was published in a volume dedicated to the 100th anniversary of Ludwig Boltzmann’s death. The purpose of the study of interaction clusters is a better understanding of the connections between large systems of interacting particles and the Boltzmann equation. For this issue we refer to [2], [19], [3] (see [7], [16] for recent progress). On the other hand, it was discovered in the engineering community that the dynamics of a rarefied gas can be approximated sufficiently well by a stochastic system of particles. The corresponding numerical tool is called direct simulation Monte Carlo (DSMC) method (cf. [1]). The rigorous connection between DSMC and the Boltzmann equation was established in [20]. In the spatially homogeneous case the basic version of DSMC reduces to the “Kac model” introduced in [8]. We refer to [13] for an extensive presentation of recent results concerning this model. The main difference between the billiard model and the stochastic model is the treatment of collisions. On the one hand, there are deterministic collisions between the billiard balls. On the other hand, collisions are generated as random events according to an appropriate collision frequency, which is determined by the intermolecular potential.

In [15] we studied models with deterministic collisions and provided an analytic description of the cluster size distribution in terms of the solution of the Boltzmann equation. The derivation was based on heuristic arguments following the approach via the Boltzmann-Grad limit. In this paper we study spatially homogeneous models with stochastic collisions. More precisely, we consider a stochastic particle model governed by an arbitrary binary interaction kernel. We establish a kinetic equation for the distribution of interaction clusters. Under some additional assumptions a recursive representation of the solution is found. In the Boltzmann case, the analytic expansion of [15] is recovered. For particular choices of the interaction kernel (including the Boltzmann case) several explicit formulas are obtained. These formulas are confirmed by numerical experiments. The experiments are also used to illustrate various conjectures and open problems.

The paper is organized as follows. The stochastic model is introduced in Section 2. The kinetic equation and properties of its solution are studied in Section 3. The particular case of Boltzmann interactions is considered in Section 4. Finally, comments on the results and open problems are given in Section 5.

2 Stochastic model

We consider a system of particles, which evolves according to a binary interaction kernel. During the evolution, interacting particles are combined into clusters. More precisely, we introduce a pure jump process of the form

$$\zeta(t) = \left(\zeta_k(t), k = 1, \dots, N(t) \right) \quad t \geq 0, \quad (2.1)$$

where the components $\zeta_k(t)$ are called clusters and $N(t)$ is the number of clusters. The state space of the process (2.1) is

$$\mathcal{Z} = \cup_{N=1}^{\infty} \mathbb{Z}^N, \quad \text{where} \quad \mathbb{Z} = \cup_{x=1}^{\infty} \{x\} \times \mathbb{V}^x \quad (2.2)$$

and \mathbb{V} is a locally compact separable metric space. The space (2.2) is called single cluster state space. Each cluster

$$z = (x, v_1, \dots, v_x) \in \mathbb{Z} \quad (2.3)$$

consists of a number (the cluster size) and a family of particles. The space \mathbb{V} is called single particle state space. The generator of the process (2.1) is

$$\begin{aligned} \mathcal{A}\Phi(\bar{z}) &= \frac{1}{n} \sum_{k,l=1}^N \sum_{\alpha=1}^{x_k} \sum_{\beta=1}^{x_l} 1_{(k,\alpha) \neq (l,\beta)} \times \\ &\int_{\mathbb{V}^2} B(v_{k,\alpha}, v_{l,\beta}, d\tilde{v}, d\tilde{w}) \left[\Phi(\bar{J}(\bar{z}, k, l, \alpha, \beta, \tilde{v}, \tilde{w})) - \Phi(\bar{z}) \right], \end{aligned} \quad (2.4)$$

where

$$\bar{z} = (z_1, \dots, z_N) \in \mathcal{Z} \quad (2.5)$$

and

$$z_k = \left(x_k, (v_{k,\alpha}, \alpha = 1, \dots, x_k) \right) \quad k = 1, \dots, N. \quad (2.6)$$

The kernel B is assumed to be compactly bounded on \mathbb{V}^2 , and $n = 1, 2, \dots$ is a scaling parameter. The jump transformation \bar{J} replaces $v_{k,\alpha}$ and $v_{l,\beta}$ by \tilde{v} and \tilde{w} , respectively. In addition, if $k \neq l$, it combines the clusters z_k and z_l into one cluster.

Time evolution

According to (2.4), the process (2.1) waits in a state \bar{z} a random time, which is exponentially distributed with parameter

$$\lambda(\bar{z}) = \frac{1}{n} \sum_{k,l=1}^N \sum_{\alpha=1}^{x_k} \sum_{\beta=1}^{x_l} 1_{(k,\alpha) \neq (l,\beta)} B_1(v_{k,\alpha}, v_{l,\beta}), \quad (2.7)$$

where

$$B_1(v, w) = \int_{\mathbb{V}^2} B(v, w, d\tilde{v}, d\tilde{w}). \quad (2.8)$$

Then two index pairs $(k, \alpha) \neq (l, \beta)$ are chosen according to the probabilities

$$\frac{B_1(v_{k,\alpha}, v_{l,\beta})}{n \lambda(\bar{z})}. \quad (2.9)$$

Next a pair of particle states \tilde{v}, \tilde{w} is generated according to

$$\frac{1}{B_1(v_{k,\alpha}, v_{l,\beta})} B(v_{k,\alpha}, v_{l,\beta}, d\tilde{v}, d\tilde{w}).$$

Finally, the particles jump from the states $v_{k,\alpha}, v_{l,\beta}$ into the states \tilde{v}, \tilde{w} and (if $k \neq l$) the corresponding clusters are combined.

Initial state

The initial state of the process (2.1) is

$$\zeta(0) = \left((1, v_1(0)), \dots, (1, v_n(0)) \right), \quad (2.10)$$

where the particles $v_i(0)$, $i = 1, \dots, n$, are independent and identically distributed according to some probability measure π on \mathbb{V} .

3 Kinetic equation

Here we study the limiting (as $n \rightarrow \infty$) kinetic equation for the cluster distribution. First a heuristic derivation of the equation is given. Then some general properties of the solution are discussed. Finally, more specific properties are obtained under certain restrictions on the interaction kernel.

3.1 Derivation of the equation

We introduce a kernel q_2 from $\mathbb{Z} \times \mathbb{Z}$ to \mathbb{Z} , which transforms two clusters into one cluster, and a kernel q_1 on \mathbb{Z} , which changes just one cluster. The kernel q_2 is defined as (cf. (2.2), (2.6))

$$q_2(z_1, z_2, d\xi) = \sum_{\alpha=1}^{x_1} \sum_{\beta=1}^{x_2} \int_{\mathbb{V}^2} B(v_{1,\alpha}, v_{2,\beta}, d\tilde{v}, d\tilde{w}) \delta_{J(z_1, z_2, \alpha, \beta, \tilde{v}, \tilde{w})}(d\xi), \quad (3.1)$$

where

$$J(z_1, z_2, \alpha, \beta, \tilde{v}, \tilde{w}) = \left(x_1 + x_2, (v'_i, i = 1, \dots, x_1 + x_2) \right) \quad (3.2)$$

and

$$v'_i = \begin{cases} v_{1,i}, & \text{if } i = 1, \dots, x_1, \quad i \neq \alpha, \\ \tilde{v}, & \text{if } i = \alpha, \\ v_{2,j}, & \text{if } i = x_1 + j, \quad j = 1, \dots, x_2, \quad j \neq \beta, \\ \tilde{w}, & \text{if } i = x_1 + \beta. \end{cases} \quad (3.3)$$

The kernel q_1 is defined as (cf. (2.3))

$$q_1^{(n)}(z, d\xi) = \frac{1}{n} \sum_{\alpha, \beta=1}^x 1_{\alpha \neq \beta} \int_{\mathbb{V}^2} B(v_\alpha, v_\beta, d\tilde{v}, d\tilde{w}) \delta_{J_1(z, \alpha, \beta, \tilde{v}, \tilde{w})}(d\xi), \quad (3.4)$$

where J_1 replaces v_α, v_β by \tilde{v}, \tilde{w} . According to (3.1) and (3.4), the generator (2.4) takes the form

$$\begin{aligned} (\mathcal{A}\Phi)(\bar{z}) &= \frac{1}{n} \sum_{k, l=1}^N 1_{k \neq l} \int_{\mathbb{Z}} q_2(z_k, z_l, d\xi) \left[\Phi(\bar{J}_2(\bar{z}, k, l, \xi)) - \Phi(\bar{z}) \right] + \\ &\quad \sum_{k=1}^N \int_{\mathbb{Z}} q_1^{(n)}(z_k, d\xi) \left[\Phi(\bar{J}_1(\bar{z}, k, \xi)) - \Phi(\bar{z}) \right], \end{aligned}$$

where the jump transformation \bar{J}_2 replaces the clusters z_k, z_l by ξ , and the jump transformation \bar{J}_1 replaces the cluster z_k by ξ .

The starting point for the derivation of the limiting equation (for $n \rightarrow \infty$) is the martingale representation for Markov processes

$$\Phi(\zeta(t)) = \Phi(\zeta(0)) + \int_0^t (\mathcal{A}\Phi)(\zeta(s)) ds + R^{(n)}(t). \quad (3.5)$$

For test functions of the form (cf. (2.5))

$$\Phi(\bar{z}) = \frac{1}{n} \sum_{k=1}^N \psi(z_k),$$

one obtains

$$\Phi(\zeta(t)) = \int_{\mathbb{Z}} \psi(z) \mu^{(n)}(t, dz) \quad (3.6)$$

and

$$\begin{aligned} (\mathcal{A}\Phi)(\zeta(t)) &= \\ &\quad \int_{\mathbb{Z}} \int_{\mathbb{Z}} \mu^{(n)}(t, dz_1) \mu^{(n)}(t, dz_2) \int_{\mathbb{Z}} q_2(z_1, z_2, d\xi) \left[\psi(\xi) - \psi(z_1) - \psi(z_2) \right] + \\ &\quad \int_{\mathbb{Z}} \mu^{(n)}(t, dz) \int_{\mathbb{Z}} q_1^{(n)}(z, d\xi) \left[\psi(\xi) - \psi(z) \right] + R_1^{(n)}(t), \end{aligned} \quad (3.7)$$

where $\mu^{(n)}$ denotes the empirical measure of the process (2.1). If there exists a deterministic limit

$$\nu(t, dz) = \lim_{n \rightarrow \infty} \mu^{(n)}(t, dz)$$

and the terms $R^{(n)}, R_1^{(n)}, q_1^{(n)}$ vanish, then it follows from (3.4), (3.5), (3.6) and (3.7) that ν satisfies the equation

$$\begin{aligned} \frac{d}{dt} \int_{\mathbb{Z}} \psi(z) \nu(t, dz) = & \quad (3.8) \\ & \int_{\mathbb{Z}} \int_{\mathbb{Z}} \nu(t, dz_1) \nu(t, dz_2) \int_{\mathbb{Z}} q_2(z_1, z_2, d\xi) \left[\psi(\xi) - \psi(z_1) - \psi(z_2) \right]. \end{aligned}$$

With the kernel (3.1), equation (3.8) takes the form

$$\begin{aligned} \frac{d}{dt} \int_{\mathbb{Z}} \psi(z) \nu(t, dz) = & \int_{\mathbb{Z}} \int_{\mathbb{Z}} \nu(t, dz_1) \nu(t, dz_2) \times & (3.9) \\ & \sum_{\alpha=1}^{x_1} \sum_{\beta=1}^{x_2} \int_{\mathbb{V}^2} B(v_{1,\alpha}, v_{2,\beta}, d\tilde{v}, d\tilde{w}) \left[\psi(J(z_1, z_2, \alpha, \beta, \tilde{v}, \tilde{w})) - \psi(z_1) - \psi(z_2) \right], \end{aligned}$$

where J is defined in (3.2), (3.3). According to (2.10), the initial condition is

$$\nu_1(0, dv) = \pi(dv), \quad \nu_x(0, dv_1, \dots, dv_x) = 0, \quad x \geq 2, \quad (3.10)$$

where ν_x denotes the restriction of ν to \mathbb{V}^x .

Remark 3.1 *Coagulation processes with very general clusters (elements of a measurable space) were studied in [14]. Our model is covered by those results, when putting $q_1^{(n)} = 0$ (cf. (3.4)). However, the convergence proof in [14] is rather sophisticated so that any extension does need care. On the other hand, the results concerning the limiting equation can be used, since equation (3.8) is identical with the differentiated form of equation (2.2) in [14].*

The general theory from [4], which includes single cluster transformation kernels q_1 , can be applied to our model. Note that the state space (2.2) is a locally compact separable metric space. Equation (3.8) is recovered from equation (2.19) in [4]. However, the case of vanishing kernels has not been considered there. Moreover, the important case of the multiplicative kernel is not covered by the assumptions.

3.2 General properties

The following results from [14] apply to equation (3.9). Let C be a quantity conserved during cluster coagulation, which means (cf. (2.2), (3.1))

$$C(\xi) = C(z_1) + C(z_2) \quad \text{a.s. with respect to } q_2(z_1, z_2, d\xi), \quad \text{for all } z_1, z_2 \in \mathbb{Z}. \quad (3.11)$$

Assume (cf. (2.8))

$$2 \sum_{\alpha=1}^{x_1} \sum_{\beta=1}^{x_2} B_1(v_{1,\alpha}, v_{2,\beta}) \leq C(z_1) C(z_2) \quad \forall z_1, z_2 \in \mathbb{Z} \quad (3.12)$$

and (cf. (3.10))

$$\int_{\mathbb{V}} C(1, v)^2 \pi(dv) < \infty. \quad (3.13)$$

■ **Theorem 2.1**

There exists a unique maximal strong solution ν , that is such that

$$\int_0^t \int_{\mathbb{Z}} C(z)^2 \nu(s, dz) < \infty \quad \forall t \in [0, T(\pi)),$$

where

$$T(\pi) \geq \left[\int_{\mathbb{V}} C(1, v)^2 \pi(dv) \right]^{-1}. \quad (3.14)$$

Moreover, this solution is conservative, that is

$$\int_{\mathbb{Z}} C(z) \nu(t, dz) = \int_{\mathbb{Z}} C(z) \nu(0, dz) = \int_{\mathbb{V}} C(1, v) \pi(dv) \quad \forall t \in [0, T(\pi)). \quad (3.15)$$

■ **Proposition 2.9**

Let ψ be a measurable function such that

$$|\psi(z)| \leq \gamma (1 + C(z)) \quad \forall z \in \mathbb{Z} \quad (3.16)$$

and

$$|\psi(\xi) - \psi(z_1) - \psi(z_2)| \leq \gamma \quad \text{a.s. w. r. to } q_2(z_1, z_2, d\xi) \quad \forall z_1, z_2 \in \mathbb{Z}, \quad (3.17)$$

for some $\gamma > 0$. Then equation (3.9) holds for ψ and $t \in [0, T(\pi))$. In particular, assumptions (3.16) and (3.17) are satisfied if ψ is bounded.

■ **Theorem 2.2**

Assume

$$\varepsilon C(z_1) C(z_2) \leq 2 \sum_{\alpha=1}^{x_1} \sum_{\beta=1}^{x_2} B_1(v_{1,\alpha}, v_{2,\beta}) \quad \forall z_1, z_2 \in \mathbb{Z}, \quad (3.18)$$

for some $\varepsilon > 0$. Then ν (provided by Theorem 2.1) is the maximal conservative solution and

$$T(\pi) \leq \left[\varepsilon \int_{\mathbb{V}} C(1, v)^2 \pi(dv) \right]^{-1}. \quad (3.19)$$

Example 3.2 *The quantity*

$$C(z) = ax \quad z \in \mathbb{Z}, \quad (3.20)$$

where $a > 0$, is conserved during cluster coagulation (cf. (3.2), (3.11)). Assumption (3.12) is equivalent to

$$B_1(v, w) \leq \frac{a^2}{2} \quad \forall v, w \in \mathbb{V}. \quad (3.21)$$

Assumption (3.13) is fulfilled. Thus, if B_1 satisfies (3.21), then (3.14) implies

$$T(\pi) \geq \frac{1}{a^2}. \quad (3.22)$$

If

$$\gamma_1 \leq B_1(v, w) \leq \gamma_2 \quad \forall v, w \in \mathbb{V}, \quad (3.23)$$

for some $\gamma_1, \gamma_2 > 0$, then assumption (3.18) is fulfilled with $\varepsilon = 2\gamma_1/a^2$. Thus, it follows from (3.19) and (3.22) that

$$\frac{1}{2\gamma_2} \leq T(\pi) \leq \frac{1}{2\gamma_1}. \quad (3.24)$$

Next we introduce several quantities based on the solution ν of equation (3.9). Later we will derive specific equations and explicit formulas for some of these quantities. We define the symmetrized measures ν^{sym} via

$$\int_{\mathbb{Z}} \psi(z) \nu^{\text{sym}}(t, dz) = \int_{\mathbb{Z}} \psi^{\text{sym}}(z) \nu(t, dz), \quad (3.25)$$

where (cf. (2.3))

$$\psi^{\text{sym}}(z) = \frac{1}{x!} \sum_{p \in \mathcal{P}(x)} \psi(x, v_{p(1)}, \dots, v_{p(x)}) \quad \forall z \in \mathbb{Z},$$

$\mathcal{P}(x)$ denotes the set of permutations of $\{1, \dots, x\}$ and ψ is an arbitrary bounded measurable function on \mathbb{Z} . We introduce the probability distributions of particles in clusters of a given size,

$$f_x(t, dv_1, \dots, dv_x) = \frac{1}{c(t, x)} \nu_x^{\text{sym}}(t, dv_1, \dots, dv_x), \quad (3.26)$$

where

$$c(t, x) = \int_{\mathbb{V}^x} \nu_x^{\text{sym}}(t, dv_1, \dots, dv_x) = \int_{\mathbb{V}^x} \nu_x(t, dv_1, \dots, dv_x), \quad (3.27)$$

and the corresponding marginals

$$f_{x,k}(t, dv_1, \dots, dv_k), \quad x = 1, 2, \dots, \quad k = 1, \dots, x. \quad (3.28)$$

Finally, we introduce the measures

$$f(t, dv) = \sum_{x=1}^{\infty} x c(t, x) f_{x,1}(t, dv) \quad (3.29)$$

and the functions (moments)

$$m_k(t) = \sum_{x=1}^{\infty} x^k c(t, x), \quad k = 0, 1, 2, \dots \quad (3.30)$$

Note that

$$m_0(t) = \nu(t, \mathbb{Z}), \quad m_1(t) = f(t, \mathbb{V}). \quad (3.31)$$

3.2.1 Total velocity distribution

Assume that the conserved quantity C is such that

$$x \leq \gamma (1 + C(z)) \quad \forall z \in \mathbb{Z}, \quad (3.32)$$

for some $\gamma > 0$. Consider test functions of the form (cf. (2.3))

$$\psi(z) = \sum_{\alpha=1}^x \varphi(v_\alpha), \quad (3.33)$$

where φ is a bounded measurable function on \mathbb{V} . It follows from (3.25), (3.29) and the symmetry of the functions (3.33) that

$$\int_{\mathbb{Z}} \psi(z) \nu(t, dz) = \int_{\mathbb{Z}} \psi(z) \nu^{\text{sym}}(t, dz) = \int_{\mathbb{V}} \varphi(v) f(t, dv). \quad (3.34)$$

Moreover, one obtains

$$\begin{aligned} & \int_{\mathbb{Z}} \int_{\mathbb{Z}} \nu(t, dz_1) \nu(t, dz_2) \times \\ & \quad \sum_{\alpha=1}^{x_1} \sum_{\beta=1}^{x_2} \int_{\mathbb{V}^2} B(v_{1,\alpha}, v_{2,\beta}, d\tilde{v}, d\tilde{w}) \left[\varphi(\tilde{v}) + \varphi(\tilde{w}) - \varphi(v_{1,\alpha}) - \varphi(v_{2,\beta}) \right] = \\ & \quad \sum_{x=1}^{\infty} \sum_{y=1}^{\infty} \int_{\mathbb{V}^x} \nu_x^{\text{sym}}(t, dv_1, \dots, dv_x) \int_{\mathbb{V}^y} \nu_y^{\text{sym}}(t, dw_1, \dots, dw_y) \times \\ & \quad \sum_{\alpha=1}^x \sum_{\beta=1}^y \int_{\mathbb{V}^2} B(v_\alpha, w_\beta, d\tilde{v}, d\tilde{w}) \left[\varphi(\tilde{v}) + \varphi(\tilde{w}) - \varphi(v_\alpha) - \varphi(w_\beta) \right] \\ & = \int_{\mathbb{V}} f(t, dv) \int_{\mathbb{V}} f(t, dw) \int_{\mathbb{V}^2} B(v, w, d\tilde{v}, d\tilde{w}) \left[\varphi(\tilde{v}) + \varphi(\tilde{w}) - \varphi(v) - \varphi(w) \right]. \end{aligned} \quad (3.35)$$

Condition (3.16) is satisfied, according to (3.32). Condition (3.17) is fulfilled. Thus, equation (3.9) holds for the functions (3.33) and $t \in [0, T(\pi))$. According to (3.34) and (3.35), equation (3.9) implies

$$\begin{aligned} \frac{d}{dt} \int_{\mathbb{V}} \varphi(v) f(t, dv) = & \quad (3.36) \\ & \int_{\mathbb{V}} f(t, dv) \int_{\mathbb{V}} f(t, dw) \int_{\mathbb{V}^2} B(v, w, d\tilde{v}, d\tilde{w}) \left[\varphi(\tilde{v}) + \varphi(\tilde{w}) - \varphi(v) - \varphi(w) \right]. \end{aligned}$$

The initial condition is (cf. (3.10))

$$f(0, dv) = \pi(dv). \quad (3.37)$$

3.2.2 Velocity distributions in the clusters

Consider bounded measurable test functions such that

$$\psi(y, v_1, \dots, v_y) = 0 \quad \forall y \neq x, \quad \text{for some } x = 1, 2, \dots$$

With $x_1 = x$, $x_2 = y$ and $x_1 = y$, $x_2 = x$, respectively, the “loss term” in equation (3.9) takes the form (cf. (2.8), (3.29))

$$\begin{aligned} & - \sum_{y=1}^{\infty} \int_{\mathbb{V}^x} \nu_x(t, dv_1, \dots, dv_x) \int_{\mathbb{V}^y} \nu_y^{\text{sym}}(t, dw_1, \dots, dw_y) \times & (3.38) \\ & \sum_{\alpha=1}^x \sum_{\beta=1}^y B_1(v_\alpha, w_\beta) \psi(x, v_1, \dots, v_x) - \\ & \sum_{y=1}^{\infty} \int_{\mathbb{V}^y} \nu_y^{\text{sym}}(t, dw_1, \dots, dw_y) \int_{\mathbb{V}^x} \nu_x(t, dv_1, \dots, dv_x) \times \\ & \sum_{\beta=1}^y \sum_{\alpha=1}^x B_1(w_\beta, v_\alpha) \psi(x, v_1, \dots, v_x) \\ & = -2 \int_{\mathbb{V}^x} \nu_x(t, dv_1, \dots, dv_x) \psi(x, v_1, \dots, v_x) \left(\sum_{\alpha=1}^x \int_{\mathbb{V}} B_1^{\text{sym}}(v_\alpha, w) f(t, dw) \right), \end{aligned}$$

where

$$B_1^{\text{sym}}(v, w) = \frac{1}{2} \left[B_1(v, w) + B_1(w, v) \right]. \quad (3.39)$$

According to (3.38), equation (3.9) implies

$$\begin{aligned} \frac{d}{dt} \int_{\mathbb{V}^x} \psi(x, v_1, \dots, v_x) \nu_x(t, dv_1, \dots, dv_x) = & \quad (3.40) \\ & -2 \int_{\mathbb{V}^x} \nu_x(t, dv_1, \dots, dv_x) \psi(x, v_1, \dots, v_x) \left(\sum_{\alpha=1}^x \int_{\mathbb{V}} B_1^{\text{sym}}(v_\alpha, w) f(t, dw) \right) + \end{aligned}$$

$$\sum_{y=1}^{x-1} \sum_{\alpha=1}^y \sum_{\beta=1}^{x-y} \int_{\mathbb{V}^y} \nu_y(t, dv_1, \dots, dv_y) \int_{\mathbb{V}^{x-y}} \nu_{x-y}(t, dw_1, \dots, dw_{x-y}) \times \\ \int_{\mathbb{V}^2} B(v_\alpha, w_\beta, d\tilde{v}, d\tilde{w}) \psi(J(y, v_1, \dots, v_y; x-y, w_1, \dots, w_{x-y}; \alpha, \beta, \tilde{v}, \tilde{w})).$$

The initial condition is (3.10).

3.2.3 Cluster size distribution

Consider test functions of the form $\psi(z) = \varphi(x)$ (cf. (2.3)), where φ is a bounded function on $\{1, 2, \dots\}$. One obtains (cf. (3.27))

$$\int_{\mathbb{Z}} \psi(z) \nu(t, dz) = \sum_{x=1}^{\infty} \varphi(x) c(t, x). \quad (3.41)$$

Moreover, it follows from (2.8) and (3.25) that

$$\int_{\mathbb{Z}} \int_{\mathbb{Z}} \nu(t, dz_1) \nu(t, dz_2) \times \\ \sum_{\alpha=1}^{x_1} \sum_{\beta=1}^{x_2} \int_{\mathbb{V}^2} B(v_{1,\alpha}, v_{2,\beta}, d\tilde{v}, d\tilde{w}) \left[\varphi(x_1 + x_2) - \varphi(x_1) - \varphi(x_2) \right] = \quad (3.42) \\ \int_{\mathbb{Z}} \int_{\mathbb{Z}} \nu^{\text{sym}}(t, dz_1) \nu^{\text{sym}}(t, dz_2) \times \\ \sum_{\alpha=1}^{x_1} \sum_{\beta=1}^{x_2} B_1(v_{1,\alpha}, v_{2,\beta}) \left[\varphi(x_1 + x_2) - \varphi(x_1) - \varphi(x_2) \right] \\ = \sum_{x=1}^{\infty} \sum_{y=1}^{\infty} \left[\varphi(x+y) - \varphi(x) - \varphi(y) \right] x y \int_{\mathbb{V}} \int_{\mathbb{V}} B_1(v, w) \nu_{x,1}^{\text{sym}}(t, dv) \nu_{y,1}^{\text{sym}}(t, dw).$$

According to (3.41) and (3.42), equation (3.9) implies

$$\frac{d}{dt} \sum_{x=1}^{\infty} \varphi(x) c(t, x) = \quad (3.43) \\ \sum_{x=1}^{\infty} \sum_{y=1}^{\infty} \left[\varphi(x+y) - \varphi(x) - \varphi(y) \right] x y \int_{\mathbb{V}} \int_{\mathbb{V}} B_1(v, w) \nu_{x,1}^{\text{sym}}(t, dv) \nu_{y,1}^{\text{sym}}(t, dw).$$

The initial condition is (cf. (3.10))

$$c(0, 1) = 1, \quad c(0, x) = 0, \quad x \geq 2. \quad (3.44)$$

Remark 3.3 Equation (3.43) is not an autonomous equation for $c(t, x)$. The notation (cf. (3.28))

$$K(t, x, y) = x y \int_{\mathbb{V}} \int_{\mathbb{V}} B_1(v, w) f_{x,1}(t, dv) f_{y,1}(t, dw) \quad (3.45)$$

emphasizes the analogy with Smoluchowski's coagulation equation, but the "coagulation kernel" (3.45) depends on the one-particle velocity distributions in the clusters.

According to (3.10), it follows from (3.43) that

$$\lim_{t \rightarrow 0} \frac{d}{dt} \sum_{x=1}^{\infty} \varphi(x) c(t, x) = [\varphi(2) - 2\varphi(1)] \int_{\mathbb{V}} \int_{\mathbb{V}} B_1(v, w) \pi(dv) \pi(dw)$$

and, in particular,

$$\lim_{t \rightarrow 0} \frac{d}{dt} c(t, 1) = -2 \int_{\mathbb{V}} \int_{\mathbb{V}} B_1(v, w) \pi(dv) \pi(dw).$$

According to (3.44), one obtains (cf. (3.30))

$$m_k(0) = 1 \quad \forall k. \quad (3.46)$$

With $\varphi(x) = 1$, it follows from (3.29), (3.43) and (3.46) that

$$\frac{d}{dt} m_0(t) = - \int_{\mathbb{V}} \int_{\mathbb{V}} B_1(v, w) f(t, dv) f(t, dw)$$

and

$$m_0(t) = 1 - \int_0^t \int_{\mathbb{V}} \int_{\mathbb{V}} B_1(v, w) f(s, dv) f(s, dw) ds \quad \forall t \in [0, T(\pi)]. \quad (3.47)$$

3.2.4 Gelation time

The gelation time is defined as (cf. (3.30))

$$t_{\text{gel}} = \inf \left\{ t \geq 0 : m_1(t) < 1 \right\}. \quad (3.48)$$

Lower bound

Assume that the conserved quantity satisfies (3.32). According to (3.31) and equation (3.36) (with $\varphi = 1$), one obtains

$$m_1(t) = 1 \quad \forall t \in [0, T(\pi)] \quad (3.49)$$

so that

$$t_{\text{gel}} \geq T(\pi). \quad (3.50)$$

It follows from (3.14) and (3.50) that

$$t_{\text{gel}} \geq \left[\int_{\mathbb{V}} C(1, v)^2 \pi(dv) \right]^{-1}. \quad (3.51)$$

Upper bounds

Assume that the conserved quantity satisfies (3.20). The conservation property (3.15) takes the form (3.49) so that assumptions (3.12), (3.13) and (3.18) imply

$$t_{\text{gel}} = T(\pi). \quad (3.52)$$

In particular, (3.52) is fulfilled, if B_1 satisfies (3.23) (cf. Example 3.2). In this case, it follows from (3.24) that

$$t_{\text{gel}} \leq \frac{1}{2\gamma_1}. \quad (3.53)$$

Next we use an equation obtained in the previous subsection in order to derive another upper bound for the gelation time.

Remark 3.4 *If (cf. (3.36), (3.37))*

$$f(t, dv) = \pi(dv) \quad \forall t \in [0, T(\pi)], \quad (3.54)$$

then the parameter (2.7) of the waiting time between collisions satisfies

$$\frac{1}{n} \sum_{i,j=1}^n 1_{i \neq j} B_1(v_i, v_j) \sim n \int_{\mathbb{V}} \int_{\mathbb{V}} B_1(v, w) \pi(dv) \pi(dw).$$

Thus, the asymptotic mean free time for one particle is

$$t_{\text{mf}} = \left[2 \int_{\mathbb{V}} \int_{\mathbb{V}} B_1(v, w) \pi(dv) \pi(dw) \right]^{-1}. \quad (3.55)$$

Under the assumption (3.54), the average number of clusters (3.47) takes the form

$$m_0(t) = 1 - \frac{t}{2t_{\text{mf}}} \quad \forall t \in [0, T(\pi)]. \quad (3.56)$$

One obtains

$$T(\pi) \leq 2t_{\text{mf}}, \quad (3.57)$$

as a consequence of (3.56) and the non-negativity of m_0 . The function

$$B_1^{(\gamma_1, \gamma_2)}(v, w) = \begin{cases} \gamma_1 & , \text{ if } B_1(v, w) \leq \gamma_1, \\ \gamma_2 & , \text{ if } B_1(v, w) \geq \gamma_2, \\ B_1(v, w), & \text{ otherwise,} \end{cases}$$

satisfies (3.23) so that (3.52) holds. Thus, the estimate (3.57) implies

$$t_{\text{gel}}^{(\gamma_1, \gamma_2)} \leq \left[\int_{\mathbb{V}} \int_{\mathbb{V}} B_1^{(\gamma_1, \gamma_2)}(v, w) \pi(dv) \pi(dw) \right]^{-1}. \quad (3.58)$$

The right-hand side of (3.58) is decreasing with $\gamma_2 \rightarrow \infty$ and increasing with $\gamma_1 \rightarrow 0$ (but staying finite, in contrast to (3.53)). Similar behaviour is expected for the left-hand side (though we are not aware of any rigorous results). This suggests the conjecture

$$t_{\text{gel}} \leq 2t_{\text{mf}}. \quad (3.59)$$

3.3 Specifications

Under certain restrictions on the interaction kernel B and the initial velocity distribution π , we construct a recurrent representation for the solution of equation (3.40) on the interval $[0, T(\pi))$.

Velocity distribution among singletons

For $x = 1$, equation (3.40) takes the form

$$\frac{d}{dt} \int_{\mathbb{V}} \psi(1, v) \nu_1(t, dv) = -2 \int_{\mathbb{V}} \nu_1(t, dv) \psi(1, v) B_2(t, v), \quad (3.60)$$

where (cf. (2.8), (3.36), (3.39))

$$B_2(t, v) = \int_{\mathbb{V}} B_1^{\text{sym}}(v, w) f(t, dw), \quad t \geq 0. \quad (3.61)$$

When removing the test functions, it follows from (3.10) and (3.60) that

$$\nu_1(t, dv) = \pi(dv) \exp\left(-2 \int_0^t B_2(s, v) ds\right). \quad (3.62)$$

3.3.1 Invertible collision transformations

Here we assume that the kernel B satisfies the condition

$$\begin{aligned} \int_{\mathbb{V}} dv \int_{\mathbb{V}} dw \int_{\mathbb{V}} \int_{\mathbb{V}} B(v, w, d\tilde{v}, d\tilde{w}) \Psi_1(v, w) \Psi_2(\tilde{v}, \tilde{w}) = \\ \int_{\mathbb{V}} dv \int_{\mathbb{V}} dw \int_{\mathbb{V}} \int_{\mathbb{V}} B(v, w, d\tilde{v}, d\tilde{w}) \Psi_1(\tilde{v}, \tilde{w}) \Psi_2(v, w), \end{aligned} \quad (3.63)$$

for any measurable functions Ψ_1, Ψ_2 such that the integrals are finite. Moreover, we assume existence of densities,

$$\nu_x(t, dv_1, \dots, dv_x) = \nu_x(t, v_1, \dots, v_x) dv_1 \dots dv_x \quad \forall x \geq 1, \quad (3.64)$$

which are denoted by the same symbols. A strong form of equation (3.36) for the total velocity distribution is obtained, namely

$$\frac{\partial}{\partial t} f(t, v) = 2 \int_{\mathbb{V}} dw \int_{\mathbb{V}^2} B(v, w, d\tilde{v}, d\tilde{w}) \left[f(t, \tilde{v}) f(t, \tilde{w}) - f(t, v) f(t, w) \right]. \quad (3.65)$$

The gain term at the right-hand side of (3.40) takes the form

$$\begin{aligned} \sum_{y=1}^{x-1} \sum_{\alpha=1}^y \sum_{\beta=1}^{x-y} \int_{\mathbb{V}^y} dv_1 \dots dv_y \int_{\mathbb{V}^{x-y}} dw_1 \dots dw_{x-y} \times \\ \int_{\mathbb{V}^2} B(v_\alpha, w_\beta, d\tilde{v}, d\tilde{w}) \nu_y(t, \tilde{J}(v_1, \dots, v_y; \alpha, \tilde{v})) \times \\ \nu_{x-y}(t, \tilde{J}(w_1, \dots, w_{x-y}; \beta, \tilde{w})) \psi(x, v_1, \dots, v_y, w_1, \dots, w_{x-y}), \end{aligned} \quad (3.66)$$

where $\tilde{J}(v_1, \dots, v_y; \alpha, \tilde{v})$ replaces v_α by \tilde{v} . When removing the test functions, it follows from (3.40) and (3.66) that

$$\begin{aligned} \frac{\partial}{\partial t} \nu_x(t, v_1, \dots, v_x) &= -2 \nu_x(t, v_1, \dots, v_x) \left(\sum_{\alpha=1}^x B_2(t, v_\alpha) \right) + \sum_{y=1}^{x-1} \sum_{\alpha=1}^y \sum_{\beta=1}^{x-y} \quad (3.67) \\ &\int_{\mathbb{V}^2} B(v_\alpha, v_{y+\beta}, d\tilde{v}, d\tilde{w}) \nu_y(t, \tilde{J}(v_1, \dots, v_y; \alpha, \tilde{v})) \nu_{x-y}(t, \tilde{J}(v_{y+1}, \dots, v_x; \beta, \tilde{w})). \end{aligned}$$

With $g_0 = 0$ (cf. (3.10)) and

$$\begin{aligned} a(t) &= -2 \left(\sum_{\alpha=1}^x B_2(t, v_\alpha) \right), \\ b(t) &= \sum_{y=1}^{x-1} \sum_{\alpha=1}^y \sum_{\beta=1}^{x-y} \int_{\mathbb{V}^2} B(v_\alpha, v_{y+\beta}, d\tilde{v}, d\tilde{w}) \times \\ &\nu_y(t, \tilde{J}(v_1, \dots, v_y; \alpha, \tilde{v})) \nu_{x-y}(t, \tilde{J}(v_{y+1}, \dots, v_x; \beta, \tilde{w})), \end{aligned}$$

one obtains from (3.67) and Remark 3.5 the system of equations

$$\begin{aligned} \nu_x(t, v_1, \dots, v_x) &= \int_0^t ds \exp \left(-2 \sum_{i=1}^x \int_s^t B_2(u, v_i) du \right) \times \\ &\sum_{y=1}^{x-1} \sum_{\alpha=1}^y \sum_{\beta=1}^{x-y} \int_{\mathbb{V}^2} B(v_\alpha, v_{y+\beta}, d\tilde{v}, d\tilde{w}) \times \quad (3.68) \\ &\nu_y(s, \tilde{J}(v_1, \dots, v_y; \alpha, \tilde{v})) \nu_{x-y}(s, \tilde{J}(v_{y+1}, \dots, v_x; \beta, \tilde{w})), \end{aligned}$$

where $x \geq 2$ and ν_1 is given in (3.62).

Remark 3.5 *The equation*

$$\frac{d}{dt} g(t) = a(t) g(t) + b(t), \quad g(0) = g_0,$$

has the solution

$$g(t) = \exp \left(\int_0^t a(s) ds \right) \left[\int_0^t \exp \left(- \int_0^s a(u) du \right) b(s) ds + g_0 \right].$$

3.3.2 Invariance condition

Let (3.63) and (3.64) be fulfilled. Moreover, we assume that B and π are such that (cf. (3.61))

$$\begin{aligned} &\int_{\mathbb{V}^2} B(v_1, v_2, d\tilde{v}, d\tilde{w}) \pi(\tilde{v}) \pi(\tilde{w}) \times \\ &\exp \left(-2 \int_0^s du \left[B_2(u, \tilde{v}) + B_2(u, \tilde{w}) \right] \right) \varphi(\tilde{v}, \tilde{w}) = \quad (3.69) \\ &\pi(v_1) \pi(v_2) \exp \left(-2 \int_0^s du \left[B_2(u, v_1) + B_2(u, v_2) \right] \right) \times \\ &\int_{\mathbb{V}^2} B(v_1, v_2, d\tilde{v}, d\tilde{w}) \varphi(\tilde{v}, \tilde{w}), \end{aligned}$$

for all $s \geq 0$, where φ is any measurable function such the integrals are finite. We show by induction that, for $x = 1, 2, \dots$,

$$\nu_x(t, v_1, \dots, v_x) = t^{x-1} \exp\left(-2 \sum_{i=1}^x \int_0^t B_2(u, v_i) du\right) \tilde{\nu}_x(v_1, \dots, v_x) \prod_{i=1}^x \pi(v_i), \quad (3.70)$$

where

$$\begin{aligned} \tilde{\nu}_x(v_1, \dots, v_x) &= \frac{1}{x-1} \sum_{y=1}^{x-1} \sum_{\alpha=1}^y \sum_{\beta=1}^{x-y} \int_{\mathbb{V}^2} B(v_\alpha, v_{y+\beta}, d\tilde{v}, d\tilde{w}) \times \\ &\quad \tilde{\nu}_y(\tilde{J}(v_1, \dots, v_y; \alpha, \tilde{v})) \tilde{\nu}_{x-y}(\tilde{J}(v_{y+1}, \dots, v_x; \beta, \tilde{w})), \quad x \geq 2, \\ \tilde{\nu}_1(v) &= 1. \end{aligned} \quad (3.71)$$

Indeed, for $x = 1$, representation (3.70) is a consequence of (3.62). For $x \geq 2$, it follows from (3.68), the induction hypothesis and assumption (3.69) that

$$\begin{aligned} \nu_x(t, v_1, \dots, v_x) &= \sum_{y=1}^{x-1} \sum_{\alpha=1}^y \sum_{\beta=1}^{x-y} \exp\left(-2 \sum_{i=1}^x \int_0^t B_2(u, v_i) du\right) \prod_{i=1}^x \pi(v_i) \int_0^t s^{x-2} ds \times \\ &\quad \int_{\mathbb{V}^2} B(v_\alpha, v_{y+\beta}, d\tilde{v}, d\tilde{w}) \tilde{\nu}_y(\tilde{J}(v_1, \dots, v_y; \alpha, \tilde{v})) \tilde{\nu}_{x-y}(\tilde{J}(v_{y+1}, \dots, v_x; \beta, \tilde{w})), \end{aligned}$$

which implies (3.70).

In particular, one obtains

$$\tilde{\nu}_2(v_1, v_2) = B_1(v_1, v_2) \quad (3.72)$$

and

$$\begin{aligned} \nu_2(t, v_1, v_2) &= t \exp\left(-2 \int_0^t [B_2(u, v_1) + B_2(u, v_2)] du\right) B_1(v_1, v_2) \pi(v_1) \pi(v_2). \end{aligned} \quad (3.73)$$

Moreover, it follows from (3.71) and (3.72) that

$$\begin{aligned} 2 \tilde{\nu}_3(v_1, v_2, v_3) &= \int_{\mathbb{V}^2} B(v_1, v_2, d\tilde{v}, d\tilde{w}) B_1(\tilde{w}, v_3) + \int_{\mathbb{V}^2} B(v_1, v_3, d\tilde{v}, d\tilde{w}) B_1(v_2, \tilde{w}) + \\ &\quad \int_{\mathbb{V}^2} B(v_1, v_3, d\tilde{v}, d\tilde{w}) B_1(\tilde{v}, v_2) + \int_{\mathbb{V}^2} B(v_2, v_3, d\tilde{v}, d\tilde{w}) B_1(v_1, \tilde{v}). \end{aligned} \quad (3.74)$$

Example 3.6 Consider a modification of the kernel B , namely the “unitary collision transformation” (cf. (2.8))

$$B^u(v, w, d\tilde{v}, d\tilde{w}) = B_1(v, w) \delta_v(d\tilde{v}) \delta_w(d\tilde{w}). \quad (3.75)$$

Both the invertibility condition (3.63) and the invariance condition (3.69) are fulfilled for the kernel (3.75) and any π . The representation (3.71) implies

$$\tilde{\nu}_x^u(v_1, \dots, v_x) = \frac{1}{x-1} \sum_{y=1}^{x-1} \tilde{\nu}_y^u(v_1, \dots, v_y) \tilde{\nu}_{x-y}^u(v_{y+1}, \dots, v_x) \left(\sum_{\alpha=1}^y \sum_{\beta=1}^{x-y} B_1(v_\alpha, v_{y+\beta}) \right), \quad (3.76)$$

where $x \geq 2$ and $\tilde{\nu}_1^u(v) = 1$. In particular, one obtains $\tilde{\nu}_2^u = B_1$ and

$$2 \tilde{\nu}_3^u(v_1, v_2, v_3) = B_1(v_2, v_3) \left[B_1(v_1, v_2) + B_1(v_1, v_3) \right] + B_1(v_1, v_2) \left[B_1(v_1, v_3) + B_1(v_2, v_3) \right].$$

Note that $B_1^u = B_1$ and $f^u(t) = \pi$, according to (3.36) and (3.37). Thus, if $f(t) = \pi$, then one obtains $B_2^u = B_2$, which implies $\nu_1 = \nu_1^u$ and $\nu_2 = \nu_2^u$ (cf. (3.62), (3.73)).

3.3.3 Constant interaction rates

Here we consider the special case, when the binary interaction rates (cf. (2.8), (2.9)) are constant,

$$B_1(v, w) = \kappa > 0. \quad (3.77)$$

According to (3.22), (3.24) and (3.55), one obtains

$$t_{\text{gel}} = t_{\text{mf}} = \frac{1}{2\kappa}. \quad (3.78)$$

Note that $T(\pi) = t_{\text{gel}}$. In the following, we consider $t \in [0, t_{\text{gel}}]$.

Cluster size distribution

When removing the test functions, equation (3.43) takes the form

$$\frac{\partial}{\partial t} c(t, x) = \sum_{y=1}^{x-1} K(y, x-y) c(t, y) c(t, x-y) - 2c(t, x) \sum_{y=1}^{\infty} K(x, y) c(t, y), \quad (3.79)$$

which is Smoluchowski's coagulation equation, with the multiplicative kernel

$$K(x, y) = \kappa x y. \quad (3.80)$$

The cluster size distribution does not depend on the collision mechanism.

Velocity distributions in the clusters

Since $f(t, \mathbb{V}) = 1$ (cf. (3.31), (3.49)), it follows from (3.61) and (3.77) that

$$B_2(t, v) = \kappa.$$

According to (3.62), one obtains

$$\nu_1(t, v) = \pi(v) \exp(-2 \kappa t). \quad (3.81)$$

The velocity distributions in the bigger clusters depend on the collision mechanism. A recurrent representation is obtained without the invertibility condition (3.63) and the invariance condition (3.69).

Equation (3.40) takes the form

$$\begin{aligned} \frac{d}{dt} \int_{\mathbb{V}^x} \psi(x, v_1, \dots, v_x) \nu_x(t, dv_1, \dots, dv_x) = & \quad (3.82) \\ & -2 \kappa x \int_{\mathbb{V}^x} \nu_x(t, dv_1, \dots, dv_x) \psi(x, v_1, \dots, v_x) + \\ & \sum_{y=1}^{x-1} \sum_{\alpha=1}^y \sum_{\beta=1}^{x-y} \int_{\mathbb{V}^y} \nu_y(t, dv_1, \dots, dv_y) \int_{\mathbb{V}^{x-y}} \nu_{x-y}(t, dw_1, \dots, dw_{x-y}) \times \\ & \int_{\mathbb{V}^2} B(v_\alpha, w_\beta, d\tilde{v}, d\tilde{w}) \psi(J(y, v_1, \dots, v_y; x-y, w_1, \dots, w_{x-y}; \alpha, \beta, \tilde{v}, \tilde{w})). \end{aligned}$$

It follows from (3.82) and Remark 3.5 that

$$\begin{aligned} \int_{\mathbb{V}^x} \psi(x, v_1, \dots, v_x) \nu_x(t, dv_1, \dots, dv_x) = \int_0^t ds \exp(-2 \kappa x (t-s)) \times & \quad (3.83) \\ \sum_{y=1}^{x-1} \sum_{\alpha=1}^y \sum_{\beta=1}^{x-y} \int_{\mathbb{V}^y} \nu_y(s, dv_1, \dots, dv_y) \int_{\mathbb{V}^{x-y}} \nu_{x-y}(s, dw_1, \dots, dw_{x-y}) \times \\ \int_{\mathbb{V}^2} B(v_\alpha, w_\beta, d\tilde{v}, d\tilde{w}) \psi(J(y, v_1, \dots, v_y; x-y, w_1, \dots, w_{x-y}; \alpha, \beta, \tilde{v}, \tilde{w})). \end{aligned}$$

We show by induction that, for $x = 1, 2, \dots$,

$$\nu_x(t, dv_1, \dots, dv_x) = t^{x-1} \exp(-2 \kappa t x) A_x(dv_1, \dots, dv_x), \quad (3.84)$$

where

$$A_1(dv) = \pi(dv) \quad (3.85)$$

and

$$\begin{aligned} \int_{\mathbb{V}^x} \psi(x, v_1, \dots, v_x) A_x(dv_1, \dots, dv_x) = & \quad (3.86) \\ \frac{1}{x-1} \sum_{y=1}^{x-1} \sum_{\alpha=1}^y \sum_{\beta=1}^{x-y} \int_{\mathbb{V}^y} A_y(dv_1, \dots, dv_y) \int_{\mathbb{V}^{x-y}} A_{x-y}(dw_1, \dots, dw_{x-y}) \times \\ \int_{\mathbb{V}^2} B(v_\alpha, w_\beta, d\tilde{v}, d\tilde{w}) \psi(J(y, v_1, \dots, v_y; x-y, w_1, \dots, w_{x-y}; \alpha, \beta, \tilde{v}, \tilde{w})), \end{aligned}$$

for $x \geq 2$ and any bounded measurable function ψ . Indeed, for $x = 1$, representation (3.84) is a consequence of (3.81). For $x \geq 2$, it follows from (3.83) and the induction hypothesis that

$$\int_{\mathbb{V}^x} \psi(x, v_1, \dots, v_x) \nu_x(t, dv_1, \dots, dv_x) = \exp(-2 \kappa t x) \frac{t^{x-1}}{x-1} \times \sum_{y=1}^{x-1} \sum_{\alpha=1}^y \sum_{\beta=1}^{x-y} \int_{\mathbb{V}^y} A_y(dv_1, \dots, dv_y) \int_{\mathbb{V}^{x-y}} A_{x-y}(dw_1, \dots, dw_{x-y}) \times \int_{\mathbb{V}^2} B(v_\alpha, w_\beta, d\tilde{v}, d\tilde{w}) \psi(J(y, v_1, \dots, v_y; x-y, w_1, \dots, w_{x-y}; \alpha, \beta, \tilde{v}, \tilde{w})),$$

which implies (3.86).

Remark 3.7 According to (3.84)–(3.86), one obtains (cf. (3.27))

$$c(t, x) = t^{x-1} \exp(-2 \kappa t x) \tilde{A}_x, \tag{3.87}$$

where

$$\tilde{A}_1 = 1 \quad \text{and} \quad \tilde{A}_x = \frac{\kappa}{x-1} \sum_{y=1}^{x-1} (x-y) y \tilde{A}_{x-y} \tilde{A}_y, \quad x \geq 2. \tag{3.88}$$

The recurrent formula (3.88), with $\kappa = \frac{1}{2}$, was used in [12]. In this case, the solution of equation (3.79), with initial condition (3.44), has the form

$$\bar{c}(t, x) = t^{x-1} \exp(-t x) \frac{x^{x-2}}{x!}. \tag{3.89}$$

It holds up to the gelation time $t_{\text{gel}} = 1$ (cf. (3.78)).

The function

$$\tilde{c}(t, x) = a c(a b t, x), \quad t \geq 0, \quad x \geq 1, \quad a, b \geq 0, \tag{3.90}$$

solves equation (3.79) with the kernel $\tilde{K} = b K$ instead of K and initial condition $\tilde{c}_0 = a c_0$ instead of c_0 . According to (3.89) and (3.90), equation (3.79) has the explicit solution

$$c(t, x) = \bar{c}(2 \kappa t, x) = (2 \kappa t)^{x-1} \exp(-2 \kappa t x) \frac{x^{x-2}}{x!}. \tag{3.91}$$

When comparing (3.87) and (3.91), one obtains

$$\tilde{A}_x = (2 \kappa)^{x-1} \frac{x^{x-2}}{x!}. \tag{3.92}$$

Assumptions (3.63) and (3.69)

Under the assumptions (3.63) and (3.64), the representation (3.85), (3.86) implies

$$A_x(v_1, \dots, v_x) = \frac{1}{x-1} \sum_{y=1}^{x-1} \sum_{\alpha=1}^y \sum_{\beta=1}^{x-y} \int_{\mathbb{V}^2} B(v_\alpha, v_{y+\beta}, d\tilde{v}, d\tilde{w}) \times A_y(\tilde{J}(v_1, \dots, v_y; \alpha, \tilde{v})) A_{x-y}(\tilde{J}(v_{y+1}, \dots, v_x; \beta, \tilde{w})), \tag{3.93}$$

where $x \geq 2$. In particular, one obtains

$$A_2(v_1, v_2) = \int_{\mathbb{V}^2} B(v_1, v_2, d\tilde{v}, d\tilde{w}) \pi(\tilde{v}) \pi(\tilde{w}) \quad (3.94)$$

instead of

$$A_2(dv_1, dv_2) = \int_{\mathbb{V}} \pi(dv) \int_{\mathbb{V}} \pi(dw) B(v, w, dv_1, dv_2). \quad (3.95)$$

The relation between (3.94) and (3.95) illustrates the impact of the ‘‘invertibility condition’’.

Under the additional assumption (3.69), we show by induction that the representation (3.93) implies (cf. (3.88))

$$A_x(v_1, \dots, v_x) = \tilde{A}_x \prod_{i=1}^x \pi(v_i), \quad x = 1, 2, \dots \quad (3.96)$$

Indeed, for $x = 1$, representation (3.96) is a consequence of (3.85). For $x \geq 2$, it follows from (3.93), the induction hypothesis and (3.69) that

$$A_x(v_1, \dots, v_x) = \frac{\kappa}{x-1} \sum_{y=1}^{x-1} \sum_{\alpha=1}^y \sum_{\beta=1}^{x-y} \tilde{A}_y \tilde{A}_{x-y} \prod_{i=1}^x \pi(v_i),$$

which implies (3.96).

It follows from (3.84) and (3.96) that (cf. (3.26))

$$f_x(t, v_1, \dots, v_x) = \prod_{i=1}^x \pi(v_i), \quad x = 1, 2, \dots \quad (3.97)$$

Remark 3.8 *If the interaction rates are constant (cf. (3.77)), then property (3.97) holds for all kernels that satisfy conditions (3.63) and (3.69). In particular, the processes with and without collisions (cf. Example 3.6) are equivalent in this case.*

Next we provide an example, where assumptions (3.63) and (3.69) are not fulfilled. In this example, property (3.97) does not necessarily hold.

Example 3.9 *Consider*

$$B(v_1, v_2, d\tilde{v}, d\tilde{w}) = P(d\tilde{v}, d\tilde{w}),$$

where P is a probability measure. In this case the ‘‘post-collision’’ velocities do not depend on the ‘‘pre-collision’’ velocities. This example is the opposite extreme case compared to Example 3.6. Equation (3.36) takes the form

$$\frac{d}{dt} \int_{\mathbb{V}} \varphi(v) f(t, dv) = \int_{\mathbb{V}} P_1(dv) \varphi(v) + \int_{\mathbb{V}} P_2(dv) \varphi(v) - 2 \int_{\mathbb{V}} \varphi(v) f(t, dv),$$

where P_1 and P_2 are the marginals of P . According to Remark 3.5, one obtains

$$\int_{\mathbb{V}} \varphi(v) f(t, dv) = \exp(-2t) \int_{\mathbb{V}} \varphi(v) \pi(dv) + \frac{1 - \exp(-2t)}{2} \left[\int_{\mathbb{V}} P_1(dv) \varphi(v) + \int_{\mathbb{V}} P_2(dv) \varphi(v) \right]$$

so that

$$f(t, dv) = \exp(-2t) \pi(dv) + (1 - \exp(-2t)) \frac{P_1(dv) + P_2(dv)}{2}$$

and

$$\lim_{t \rightarrow \infty} f(t, dv) = \frac{P_1(dv) + P_2(dv)}{2}.$$

According to (3.84) and (3.95), one obtains

$$\nu_2(t, dv_1, dv_2) = t \exp(-4t) P(dv_1, dv_2)$$

so that (cf. (3.28))

$$f_{2,1}(t, dv) = \frac{P_1(dv) + P_2(dv)}{2}.$$

Both dependence and independence of the velocities in the clusters of size 2 are possible. Consider, for example,

$$P(d\tilde{v}, d\tilde{w}) = \int_{\mathbb{V}} \tilde{P}(dv) \delta_v(d\tilde{v}) \delta_v(d\tilde{w}) \quad \text{or} \quad P(d\tilde{v}, d\tilde{w}) = P_1(d\tilde{v}) P_2(d\tilde{w}),$$

where \tilde{P} , P_1 , P_2 are probability measures.

3.3.4 Multi-colour clusters

Here we consider another example, where explicit formulas are obtained both for the gelation time and for the mean free time. Moreover, the ratio of these two quantities may take any value in the interval $(0, 1]$. Consider the kernel (cf. (3.75))

$$B(v, w, d\tilde{v}, d\tilde{w}) = B_1(v, w) \delta_v(d\tilde{v}) \delta_w(d\tilde{w}), \quad (3.98)$$

where

$$B_1(v, w) = \beta(v) 1_{v=w} \quad v, w \in \mathbb{V}, \quad (3.99)$$

β is some non-negative function and \mathbb{V} is a finite set. The mean free time (3.55) takes the form

$$t_{\text{mf}} = \frac{1}{2 \sum_{v \in \mathbb{V}} \beta(v) \pi(v)^2}. \quad (3.100)$$

According to (3.76), one obtains

$$\tilde{\nu}_x(v, \dots, v) = \frac{\beta(v)}{x-1} \sum_{y=1}^{x-1} (x-y) y \tilde{\nu}_{x-y}(v, \dots, v) \tilde{\nu}_y(v, \dots, v),$$

where $x \geq 2$ and $\tilde{\nu}_1(v) = 1$, while all other quantities $\tilde{\nu}_x(v_1, \dots, v_x)$ are zero. According to (3.88) and (3.92), one obtains

$$\tilde{\nu}_x(v, \dots, v) = (2\beta(v))^{x-1} \frac{x^{x-2}}{x!}. \quad (3.101)$$

It follows from (3.61) and (3.99) that

$$B_2(\pi, v) = \beta(v) \pi(v). \quad (3.102)$$

According to (3.101) and (3.102), the solution (3.70) takes the form (cf. (3.89))

$$\begin{aligned} \nu_x(t, v, \dots, v) &= (2\beta(v) \pi(v) t)^{x-1} \exp\left(-2\beta(v) \pi(v) t x\right) \frac{x^{x-2}}{x!} \pi(v) \\ &= \pi(v) \bar{c}(2\beta(v) \pi(v) t, x), \end{aligned}$$

while all other values are zero. One obtains (cf. (3.27), (3.28))

$$c(t, x) = \sum_{v \in \mathbb{V}} \pi(v) \bar{c}(2\beta(v) \pi(v) t, x) \quad (3.103)$$

and

$$f_{x,1}(t, v) = f_x(t, v, \dots, v) = \pi(v) \frac{\bar{c}(2\beta(v) \pi(v) t, x)}{c(t, x)}. \quad (3.104)$$

It follows from (3.103) that (cf. (3.30))

$$m_1(t) = \sum_{v \in \mathbb{V}} \pi(v) \bar{m}_1(2\beta(v) \pi(v) t).$$

Thus, the gelation time (3.48) takes the form (cf. (3.89), (3.91))

$$t_{\text{gel}} = \min_{v \in \mathbb{V}} \frac{1}{2\beta(v) \pi(v)} = \frac{1}{2 \max_{v \in \mathbb{V}} \beta(v) \pi(v)}. \quad (3.105)$$

We assume

$$\max_{v \in \mathbb{V}} \beta(v) \pi(v) > 0.$$

According to (3.100) and (3.105), one obtains

$$\frac{t_{\text{gel}}}{t_{\text{mf}}} = \frac{\sum_{v \in \mathbb{V}} \beta(v) \pi(v)^2}{\max_{v \in \mathbb{V}} \beta(v) \pi(v)} \leq 1. \quad (3.106)$$

Equality in (3.106) holds if and only if

$$\beta(v) \pi(v) = b > 0, \quad \text{almost surely with respect to } \pi. \quad (3.107)$$

Note that $\frac{t_{\text{gel}}}{t_{\text{mf}}} = \frac{\mathbb{E} \xi}{\max \xi}$, for the random variable $\xi(v) = \beta(v) \pi(v)$. In particular, condition (3.107) is fulfilled if $|\mathbb{V}| = 1$. This is the only case, where the function B_1 is constant (cf. (3.99)).

On the other hand, it is of interest to find the minimal value of the quotient $\frac{t_{\text{gel}}}{t_{\text{mf}}}$. Consider $v_0 \in \mathbb{V}$, $\varepsilon \geq 0$ and

$$\pi(v) = \frac{1}{|\mathbb{V}|}, \quad \beta(v) = 1_{v=v_0} + \varepsilon 1_{v \neq v_0} \quad v \in \mathbb{V}.$$

According to (3.106), one obtains

$$\frac{t_{\text{gel}}}{t_{\text{mf}}} = \frac{1}{|\mathbb{V}|} [1 + \varepsilon (|\mathbb{V}| - 1)].$$

This expression becomes arbitrarily small, when choosing ε small and $|\mathbb{V}|$ large.

Remark 3.10 *If condition (3.107) is fulfilled, then (3.103) and (3.104) imply $c(t, x) = \bar{c}(2bt, x)$ and $f_{x,1}(t, v) = \pi(v)$. Property (3.97) does not hold, except in the one-colour case, since $f_2(t, v, w) = 0$ if $v \neq w$. The one-colour case corresponds to constant interaction rates and the kernel (3.98) satisfies conditions (3.63) and (3.69) (cf. Remark 3.8).*

4 Boltzmann interactions

Consider $\mathbb{V} = \mathbb{R}^d$, with $d \geq 2$, and

$$B(v, w, d\tilde{v}, d\tilde{w}) = \frac{1}{2} \int_{\mathbb{S}^{d-1}} de b(v, w, e) \delta_{v^*(v, w, e)}(d\tilde{v}) \delta_{w^*(v, w, e)}(d\tilde{w}), \quad (4.1)$$

where b is some non-negative integrable function,

$$v^*(v, w, e) = \frac{v + w}{2} + e \frac{\|v - w\|}{2}, \quad w^*(v, w, e) = \frac{v + w}{2} - e \frac{\|v - w\|}{2}, \quad (4.2)$$

and \mathbb{S}^{d-1} denotes the unit sphere in \mathbb{R}^d . The collision transformation (4.2) satisfies

$$\begin{aligned} v^*(v, w, e) + w^*(v, w, e) &= v + w \\ \|v^*(v, w, e) - w^*(v, w, e)\| &= \|v - w\| \\ \|v^*(v, w, e)\|^2 + \|w^*(v, w, e)\|^2 &= \|v\|^2 + \|w\|^2, \end{aligned} \quad (4.3)$$

since $\|v + w\|^2 + \|v - w\|^2 = 2(\|v\|^2 + \|w\|^2)$. Moreover, one obtains (cf., e.g., [17, p.16])

$$\int_{\mathbb{R}^d} \int_{\mathbb{R}^d} \int_{\mathbb{S}^{d-1}} \psi(v, w, v^*, w^*) de dw dv = \int_{\mathbb{R}^d} \int_{\mathbb{R}^d} \int_{\mathbb{S}^{d-1}} \psi(v^*, w^*, v, w) de dw dv, \quad (4.4)$$

for any measurable function ψ such that the integrals are finite. We assume

$$b(v, w, e) = b(v, w, -e) \quad (4.5)$$

and

$$b(v, w, e) = b(v^*, w^*, e). \quad (4.6)$$

Assumptions (4.5) and (4.6) are fulfilled, e.g., if

$$b(v, w, e) = \tilde{b}(v + w, \|v - w\|), \quad (4.7)$$

for some measurable function \tilde{b} .

The **invertibility condition** (3.63) is fulfilled, according to (4.4) and (4.6). Equation (3.65) for the total velocity distribution takes the form

$$\frac{\partial}{\partial t} f(t, v) = \int_{\mathbb{R}^d} dw \int_{\mathbb{S}^{d-1}} de b(v, w, e) \left[f(t, v^*) f(t, w^*) - f(t, v) f(t, w) \right], \quad (4.8)$$

which is the spatially homogeneous Boltzmann equation with collision kernel b . We consider a Maxwellian initial state,

$$f(0, v) = M(\sigma, v) := \frac{1}{(2\pi\sigma^2)^{\frac{d}{2}}} \exp\left(-\frac{\|v\|^2}{2\sigma^2}\right) \quad v \in \mathbb{R}^d, \quad (4.9)$$

where $\sigma > 0$ is a parameter. Note that (cf. (3.54))

$$f(t, v) = M(\sigma, v) \quad \forall t \in [0, T(\sigma)], \quad (4.10)$$

according to (4.3) and (4.8).

Properties of the Maxwellian

Here we collect some properties of the distribution (4.9). One obtains

$$\int_{\mathbb{R}^d} \|v\|^k M(\sigma, v) dv = \frac{2^{\frac{k}{2}} \Gamma(\frac{d+k}{2})}{\Gamma(\frac{d}{2})} \sigma^k, \quad k > -d. \quad (4.11)$$

Note that

$$\Gamma(x) = (x-1)\Gamma(x-1), \quad \Gamma(0.5) = \sqrt{\pi}. \quad (4.12)$$

For $k = 2, 4, 6$, expression (4.11) takes the form

$$d\sigma^2, \quad d(d+2)\sigma^4 \quad \text{and} \quad d(d+2)(d+4)\sigma^6, \quad (4.13)$$

respectively. Moreover, using the substitution $v - w = x$, $v + w = y$, one obtains

$$\begin{aligned} & \int_{\mathbb{R}^d} \int_{\mathbb{R}^d} \varphi(\|v - w\|) M(\sigma, v) M(\sigma, w) dv dw = \\ & \int_{\mathbb{R}^d} \int_{\mathbb{R}^d} \varphi(\|x\|) \frac{1}{(2\pi\sigma^2)^d} \exp\left(-\frac{\|x\|^2 + \|y\|^2}{4\sigma^2}\right) \frac{1}{2^d} dx dy \\ & = \int_{\mathbb{R}^d} \varphi(\|v\|) M(\sqrt{2}\sigma, v) dv, \end{aligned} \quad (4.14)$$

where φ is any measurable function such that the integrals are finite. Note that the transformation $(v, w) = \Psi(x, y)$ satisfies $|\det \Psi'| = \frac{1}{2^d}$. It follows from (4.11) and (4.14) that

$$\int_{\mathbb{R}^d} \int_{\mathbb{R}^d} \|v - w\|^k M(\sigma, v) M(\sigma, w) dv dw = \frac{\Gamma(\frac{d+k}{2})}{\Gamma(\frac{d}{2})} (2\sigma)^k, \quad k > -d. \quad (4.15)$$

Conserved quantities

According to (3.11) and (4.3), the functions (cf. (2.3))

$$C(z) = C_1 x + C_2 \sum_{i=1}^x \|v_i\|^2 \quad z \in \mathbb{Z},$$

where $C_1, C_2 \geq 0$, are conserved quantities with respect to the kernel (3.1).

■ Assumption (3.12) is equivalent to

$$2 B_1(v, w) \leq (C_1 + C_2 \|v\|^2) (C_1 + C_2 \|w\|^2) \quad \forall v, w \in \mathbb{R}^d, \quad (4.16)$$

where (cf. (2.8), (4.1))

$$B_1(v, w) = \frac{1}{2} \int_{\mathbb{S}^{d-1}} b(v, w, e) de. \quad (4.17)$$

■ Assumption (3.13) takes the form

$$\int_{\mathbb{R}^d} (C_1 + C_2 \|v\|^2)^2 M(\sigma, v) dv < \infty$$

and is always fulfilled.

Thus, if B_1 satisfies (4.16) and $C_1 > 0$ (cf. (3.32)), then (3.51) and (4.13) imply

$$t_{\text{gel}} \geq \left(C_1^2 + 2 C_1 C_2 d \sigma^2 + C_2^2 d (d+2) \sigma^4 \right)^{-1}. \quad (4.18)$$

Special functionals of the solution

We consider the mean one-particle energies in the clusters (cf. (3.28))

$$E_x(t) = \int_{\mathbb{R}^d} \|v\|^2 f_{x,1}(t, v) dv, \quad x = 1, 2, \dots \quad (4.19)$$

Since (cf. (3.36))

$$\int_{\mathbb{R}^d} \|v\|^2 f(t, v) dv = \int_{\mathbb{R}^d} \|v\|^2 M(\sigma, v) dv, \quad t \geq 0,$$

one obtains (cf. (3.29), (4.13))

$$\sum_{x=1}^{\infty} x c(t, x) E_x(t) = d \sigma^2.$$

We also introduce the two-particle correlation coefficients in the clusters

$$r_x(t) = \frac{\int_{\mathbb{R}^d} \int_{\mathbb{R}^d} (v_1, v_2) f_{x,2}(t, v_1, v_2) dv_1 dv_2}{E_x(t)}, \quad x = 2, 3, \dots \quad (4.20)$$

The definition (4.20) is based on the notion of the correlation coefficient

$$\frac{\mathbb{E}(\xi, \eta)}{\sqrt{\mathbb{E}\|\xi\|^2 \mathbb{E}\|\eta\|^2}},$$

where ξ and η are random vectors.

Scaling properties

Multiplication of the collision kernel by some factor leads to a corresponding time scaling of the process (cf. (2.7), (3.9), (3.90)). Under some restrictions on the collision kernel, scaling with respect to the parameter σ is also related to a certain time scaling. Indeed, the initial state (2.10) satisfies

$$v_i^{(\sigma)}(0) = \sigma v_i^{(1)}(0), \quad i = 1, \dots, n,$$

where the superscript indicates the dependence on σ . According to (4.2), one obtains

$$v^*(\sigma v, \sigma w, e) = \sigma v^*(v, w, e).$$

If (cf. (4.1))

$$b(\sigma v, \sigma w, e) = \sigma^k b(v, w, e) \quad \text{for some } k \geq 0, \quad (4.21)$$

then the process can be represented as

$$v_i^{(\sigma)}(t) = \sigma v_i^{(1)}(\sigma^k t), \quad i = 1, \dots, n, \quad t \geq 0. \quad (4.22)$$

In particular, one obtains (cf. (4.19), (4.20))

$$E_x^{(\sigma)}(t) = \sigma^2 E_x^{(1)}(\sigma^k t) \quad \text{and} \quad r_x^{(\sigma)}(t) = r_x^{(1)}(\sigma^k t).$$

4.1 Hard sphere gas

Consider N spherical particles with radius r , with uniform positions in a domain of volume V in \mathbb{R}^d ($d \geq 2$) and with velocities distributed according to a Maxwellian. The particles move and collide according to the Newtonian dynamics. This is the billiard model, which was studied in [6] and [11].

The average number of collisions of a particle on a time interval of length Δt is

$$\int_{\mathbb{R}^d} M(\sigma, v) dv \int_{\mathbb{R}^d} M(\sigma, w) dw \left(|D_{d-1}(2r)| \times \|v - w\| \Delta t \right) \times \frac{N}{V},$$

where

$$D_d(r) = \{v \in \mathbb{R}^d : \|v\| \leq r\}. \quad (4.23)$$

Thus, the **mean free time** is (cf. (4.15))

$$\begin{aligned} t_{\text{mf}}^{\text{HS}} &= \left[\frac{|D_{d-1}(2r)| N}{V} \int_{\mathbb{R}^d} \int_{\mathbb{R}^d} \|v - w\| M(\sigma, v) M(\sigma, w) dv dw \right]^{-1} \\ &= \left[\frac{|D_{d-1}(2r)| N}{V} 2\sigma \frac{\Gamma(\frac{d+1}{2})}{\Gamma(\frac{d}{2})} \right]^{-1}. \end{aligned} \quad (4.24)$$

The derivation of (4.24) assumes that

- N is sufficiently big so that the initial Maxwellian velocity distribution remains approximately valid during the time evolution;
- r is sufficiently small so that the distribution of the positions is approximately uniform;
- the volume fraction is sufficiently small so that the dynamics makes sense,

$$\frac{|D_d(r)| N}{V} \ll 1. \quad (4.25)$$

The **mean free path** is (cf. (4.11), (4.24))

$$x_{\text{mf}} = t_{\text{mf}}^{\text{HS}} \int_{\mathbb{R}^d} \|v\| M(\sigma, v) dv = \left[\sqrt{2} \frac{|D_{d-1}(2r)| N}{V} \right]^{-1}. \quad (4.26)$$

Stochastic model

We consider the collision kernel (cf. (4.1))

$$b(v, w, e) = \frac{2\gamma^{\text{HS}}}{|\mathbb{S}^{d-1}|} \|v - w\|, \quad (4.27)$$

where $\gamma^{\text{HS}} > 0$. One obtains (cf. (4.17))

$$B_1(v, w) = \gamma^{\text{HS}} \|v - w\|. \quad (4.28)$$

The mean free time (3.55) takes the form

$$t_{\text{mf}} = \left[2\gamma^{\text{HS}} \int_{\mathbb{R}^d} \int_{\mathbb{R}^d} \|v - w\| M(\sigma, v) M(\sigma, w) dv dw \right]^{-1}. \quad (4.29)$$

According to (4.24) and (4.29), one obtains

$$t_{\text{mf}} = t_{\text{mf}}^{\text{HS}}$$

if (cf. (4.26))

$$\gamma^{\text{HS}} = \frac{|D_{d-1}(2r)|N}{2V} = \frac{1}{2\sqrt{2}x_{\text{mf}}}. \quad (4.30)$$

Note that (cf. (4.12), (4.23))

$$|D_d(r)| = \frac{r^d \pi^{\frac{d}{2}}}{\Gamma(\frac{d}{2} + 1)} \quad \text{and} \quad |\mathbb{S}^{d-1}| = \frac{d \pi^{\frac{d}{2}}}{\Gamma(\frac{d}{2} + 1)}. \quad (4.31)$$

It follows from (4.24), (4.30) and (4.31) that

$$t_{\text{mf}}^{\text{HS}} = \left[\gamma^{\text{HS}} 4\sigma \frac{\Gamma(\frac{d+1}{2})}{\Gamma(\frac{d}{2})} \right]^{-1} = \left[r^{d-1} \frac{N}{V} \sigma \frac{2^d \pi^{\frac{d-1}{2}}}{\Gamma(\frac{d}{2})} \right]^{-1}. \quad (4.32)$$

The correspondence between the billiard model and the stochastic model is established via the ‘‘Boltzmann-Grad limit’’ ($\lim_{N \rightarrow \infty} r_N^{d-1} N \in (0, \infty)$), which leads to the Boltzmann equation (4.8).

Gelation time

Since $\|v - w\| \leq \frac{1}{4} + \|v - w\|^2 \leq \frac{1}{4} + 2(\|v\|^2 + \|w\|^2)$, assumption (4.16) is satisfied provided that

$$\gamma^{\text{HS}} \leq 2C_1^2 \quad \text{and} \quad 4\gamma^{\text{HS}} \leq C_1 C_2. \quad (4.33)$$

A lower bound for the gelation time is obtained via (4.18) and (4.33), while an upper bound follows from (3.59) and (4.32).

4.2 Special collision kernel

We consider the collision kernel (cf. (4.1), (4.7))

$$b(v, w, e) = \frac{2}{|\mathbb{S}^{d-1}|} \left(\kappa + \gamma \|v - w\|^2 \right), \quad (4.34)$$

where $\kappa, \gamma \geq 0$ are parameters. This is a toy model that generalizes the case of constant interaction rates ($\gamma = 0$). The model has no direct physical relevance, but (for $\kappa = 0$ and $\gamma > 0$) it is expected to be qualitatively similar to the hard sphere model (cf. (4.27)). Moreover, some explicit formulas for the velocity distributions in the clusters will be derived for the kernel (4.34).

One obtains (cf. (4.17))

$$B_1(v, w) = \kappa + \gamma \|v - w\|^2. \quad (4.35)$$

It follows from (3.61), (4.10), (4.13) and (4.35) that

$$\begin{aligned} B_2(t, v) &= \kappa + \gamma \int_{\mathbb{R}^d} M(\sigma, w) \left(\|v\|^2 - 2(v, w) + \|w\|^2 \right) dw \\ &= \kappa + \gamma (\|v\|^2 + d\sigma^2). \end{aligned} \quad (4.36)$$

The **invariance condition** (3.69) is fulfilled, since (cf. (4.3))

$$M(\sigma, v^*) M(\sigma, w^*) = M(\sigma, v) M(\sigma, w)$$

and

$$B_2(t, v^*) + B_2(t, w^*) = B_2(t, v) + B_2(t, w).$$

The mean free time (3.55) takes the form

$$t_{\text{mf}} = \frac{1}{2\kappa + 4\gamma d\sigma^2}. \quad (4.37)$$

Gelation time

Since $\|v - w\|^2 \leq 2(\|v\|^2 + \|w\|^2)$, assumption (4.16) is satisfied provided that

$$2\kappa \leq C_1^2 \quad \text{and} \quad 4\gamma \leq C_1 C_2. \quad (4.38)$$

A lower bound for the gelation time is obtained via (4.18) and (4.38), while an upper bound follows from (3.59) and (4.37).

Velocity distributions in the clusters

If $\gamma = 0$, then one obtains (cf. Remark 3.8)

$$f_x(t, v_1, \dots, v_x) = \prod_{i=1}^x M(\sigma, v_i), \quad x = 1, 2, \dots \quad (4.39)$$

In the following we assume $\gamma > 0$. Note that

$$\begin{aligned} M(\sigma, v) \exp(-2t\gamma\|v\|^2) &= \\ \frac{1}{(2\pi\sigma^2)^{\frac{d}{2}}} \exp\left(-\frac{\|v\|^2}{2}\left(\frac{1}{\sigma^2} + 4t\gamma\right)\right) &= \frac{1}{(1 + 4t\gamma\sigma^2)^{\frac{d}{2}}} M(\sigma_\gamma(t), v), \end{aligned} \quad (4.40)$$

where

$$\sigma_\gamma^2(t) = \frac{\sigma^2}{1 + 4t\gamma\sigma^2}. \quad (4.41)$$

According to (4.36) and (4.40), the representation (3.70) takes the form

$$\nu_x(t, v_1, \dots, v_x) = \frac{t^{x-1} \exp(-2tx(\kappa + d\gamma\sigma^2))}{(1 + 4t\gamma\sigma^2)^{\frac{d}{2}x}} \tilde{\nu}_x(v_1, \dots, v_x) \prod_{i=1}^x M(\sigma_\gamma(t), v_i),$$

where $\tilde{\nu}_x$ is defined in (3.71). One obtains (cf. (3.26), (3.27))

$$c(t, x) = \frac{t^{x-1} \exp(-2t x (\kappa + d\gamma\sigma^2))}{(1 + 4t\gamma\sigma^2)^{\frac{d}{2}x}} I(t, x) \quad (4.42)$$

and

$$f_x(t, v_1, \dots, v_x) = \frac{1}{I(t, x)} \tilde{\nu}_x^{\text{sym}}(v_1, \dots, v_x) \prod_{i=1}^x M(\sigma_\gamma(t), v_i), \quad (4.43)$$

where

$$I(t, x) = \int_{\mathbb{V}^x} \tilde{\nu}_x(v_1, \dots, v_x) \prod_{i=1}^x M(\sigma_\gamma(t), v_i) dv_1 \dots dv_x. \quad (4.44)$$

Clusters of size 1

According to (3.71), (4.42) and (4.43), one obtains

$$c(t, 1) = \frac{\exp(-2t(\kappa + d\gamma\sigma^2))}{(1 + 4t\gamma\sigma^2)^{\frac{d}{2}}}$$

and

$$f_1(t, v) = M(\sigma_\gamma(t), v).$$

Thus,

- the velocity distribution among clusters of size 1 is a Maxwellian with decreasing temperature (4.41).

The one-particle energy (4.19) takes the form

$$E_1(t) = d\sigma_\gamma^2(t). \quad (4.45)$$

Clusters of size 2

According to (3.72), (4.35) and (4.44), one obtains (cf. (4.13))

$$\begin{aligned} I(t, 2) &= \int_{\mathbb{R}^d} \int_{\mathbb{R}^d} (\kappa + \gamma \|v_1 - v_2\|^2) M(\sigma_\gamma(t), v_1) M(\sigma_\gamma(t), v_2) dv_1 dv_2 \\ &= \kappa + 2\gamma d\sigma_\gamma^2(t) \end{aligned}$$

so that (4.42) and (4.43) imply

$$c(t, 2) = \frac{t \exp\left(-4t(\kappa + d\gamma\sigma^2)\right)}{(1 + 4t\gamma\sigma^2)^d} \left(\kappa + 2\gamma d\sigma_\gamma^2(t)\right)$$

and

$$f_2(t, v_1, v_2) = \frac{\left(\kappa + \gamma \|v_1 - v_2\|^2\right) M(\sigma_\gamma(t), v_1) M(\sigma_\gamma(t), v_2)}{\kappa + 2\gamma d \sigma_\gamma^2(t)}. \quad (4.46)$$

The one-particle marginal is

$$f_{2,1}(t, v) = \frac{\left(\kappa + d\gamma \sigma_\gamma^2(t) + \gamma \|v\|^2\right) M(\sigma_\gamma(t), v)}{\kappa + 2\gamma d \sigma_\gamma^2(t)}.$$

Thus,

- the one-particle velocity distribution in clusters of size 2 is not a Maxwellian;
- the two velocities in clusters of size 2 are not independent.

The one-particle energy (4.19) takes the form (cf. (4.13))

$$\begin{aligned} E_2(t) &= \frac{\left(\kappa + d\gamma \sigma_\gamma^2(t)\right) d \sigma_\gamma^2(t) + \gamma d(d+2) \sigma_\gamma^4(t)}{\kappa + 2\gamma d \sigma_\gamma^2(t)} \\ &= \frac{\kappa d \sigma_\gamma^2(t) + 2\gamma d(d+1) \sigma_\gamma^4(t)}{\kappa + 2\gamma d \sigma_\gamma^2(t)}. \end{aligned} \quad (4.47)$$

Since

$$\int_{\mathbb{R}^d} \int_{\mathbb{R}^d} (v_1, v_2)^2 M(\sigma, v_1) M(\sigma, v_2) dv_1 dv_2 = d \sigma^4, \quad (4.48)$$

it follows from (4.46) that

$$\int_{\mathbb{R}^d} \int_{\mathbb{R}^d} (v_1, v_2) f_2(t, v_1, v_2) dv_1 dv_2 = \frac{-2\gamma d \sigma_\gamma^4(t)}{\kappa + 2\gamma d \sigma_\gamma^2(t)}. \quad (4.49)$$

According to (4.47) and (4.49), the two-particle correlation coefficient (4.20) takes the form

$$r_2(t) = \frac{-2\gamma d \sigma_\gamma^2(t)}{\kappa d + 2\gamma d(d+1) \sigma_\gamma^2(t)}. \quad (4.50)$$

If $\kappa = 0$, then (4.47) and (4.50) imply

$$E_2(t) = (d+1) \sigma_\gamma^2(t), \quad r_2(t) = -\frac{1}{d+1}. \quad (4.51)$$

Clusters of size 3

According to (4.1), (4.2) and (4.5), one obtains

$$\begin{aligned}
 F(v_1, v_2, v_3) &:= \int_{\mathbb{V}^2} B(v_1, v_2, d\tilde{v}, d\tilde{w}) B_1(\tilde{w}, v_3) = \\
 &\frac{1}{2} \int_{\mathbb{S}^{d-1}} de b(v_1, v_2, e) B_1(w^*(v_1, v_2, e), v_3) = \int_{\mathbb{V}^2} B(v_1, v_2, d\tilde{v}, d\tilde{w}) B_1(\tilde{v}, v_3)
 \end{aligned} \tag{4.52}$$

so that the representation (3.74) takes the form

$$2 \tilde{\nu}_3(v_1, v_2, v_3) = F(v_1, v_2, v_3) + 2 F(v_1, v_3, v_2) + F(v_2, v_3, v_1). \tag{4.53}$$

The function (4.35) satisfies (cf. (4.3))

$$B_1(v^*(v_1, v_2, e), v_3) + B_1(w^*(v_1, v_2, e), v_3) = B_1(v_1, v_3) + B_1(v_2, v_3). \tag{4.54}$$

It follows from (4.52) and (4.54) that

$$\begin{aligned}
 F(v_1, v_2, v_3) &= \frac{1}{2} \int_{\mathbb{V}^2} B(v_1, v_2, d\tilde{v}, d\tilde{w}) \left[B_1(\tilde{v}, v_3) + B_1(\tilde{w}, v_3) \right] \\
 &= \frac{1}{2} B_1(v_1, v_2) \left[B_1(v_1, v_3) + B_1(v_2, v_3) \right].
 \end{aligned}$$

Thus, (4.53) implies

$$\begin{aligned}
 \tilde{\nu}_3^{\text{sym}}(v_1, v_2, v_3) &= 2 F^{\text{sym}}(v_1, v_2, v_3) = \\
 &\frac{2}{3} \left[B_1(v_1, v_2) B_1(v_1, v_3) + B_1(v_2, v_1) B_1(v_2, v_3) + B_1(v_3, v_1) B_1(v_3, v_2) \right].
 \end{aligned} \tag{4.55}$$

According to (4.42)-(4.44) and (4.55), one obtains

$$c(t, 3) = \frac{t^2 \exp(-6 t (\kappa + d \gamma \sigma^2))}{(1 + 4 t \gamma \sigma^2)^{\frac{3d}{2}}} I(t, 3)$$

and

$$f_3(t, v_1, v_2, v_3) = \frac{1}{I(t, 3)} \tilde{\nu}_3^{\text{sym}}(v_1, v_2, v_3) \prod_{i=1}^3 M(\sigma_\gamma(t), v_i), \tag{4.56}$$

where (cf. (4.13))

$$\begin{aligned}
 \frac{1}{2} I(t, 3) &= \int_{\mathbb{V}^3} B_1(v_1, v_2) B_1(v_1, v_3) \prod_{i=1}^3 M(\sigma_\gamma(t), v_i) dv_1 dv_2 dv_3 = \\
 &\kappa^2 + 4 d \kappa \gamma \sigma_\gamma^2(t) + \\
 &\gamma^2 \int_{\mathbb{V}^3} \left(\|v_1\|^2 + \|v_2\|^2 \right) \left(\|v_1\|^2 + \|v_3\|^2 \right) \prod_{i=1}^3 M(\sigma_\gamma(t), v_i) dv_1 dv_2 dv_3 \\
 &= \kappa^2 + 4 d \kappa \gamma \sigma_\gamma^2(t) + 2 d (2 d + 1) \gamma^2 \sigma_\gamma^4(t).
 \end{aligned} \tag{4.57}$$

Since

$$\begin{aligned}
& \int_{\mathbb{R}^d} dv_2 \int_{\mathbb{R}^d} dv_3 B_1(v_1, v_2) B_1(v_1, v_3) M(\sigma, v_2) M(\sigma, v_3) = \\
& \quad \kappa^2 + 2 \kappa \gamma \left(\|v_1\|^2 + d \sigma^2 \right) + \\
& \quad \gamma^2 \int_{\mathbb{R}^d} dv_2 \int_{\mathbb{R}^d} dv_3 \left(\|v_1\|^2 + \|v_2\|^2 \right) \left(\|v_1\|^2 + \|v_3\|^2 \right) M(\sigma, v_2) M(\sigma, v_3) \\
& = \kappa^2 + 2 \kappa \gamma \left(\|v_1\|^2 + d \sigma^2 \right) + \gamma^2 \left(\|v_1\|^4 + 2 d \sigma^2 \|v_1\|^2 + d^2 \sigma^4 \right)
\end{aligned}$$

and

$$\begin{aligned}
& \int_{\mathbb{R}^d} dv_2 \int_{\mathbb{R}^d} dv_3 B_1(v_2, v_1) B_1(v_2, v_3) M(\sigma, v_2) M(\sigma, v_3) = \\
& \quad \int_{\mathbb{R}^d} dv_2 \int_{\mathbb{R}^d} dv_3 B_1(v_3, v_1) B_1(v_3, v_2) M(\sigma, v_2) M(\sigma, v_3) \\
& = \kappa^2 + \kappa \gamma \left(3 d \sigma^2 + \|v_1\|^2 \right) + \\
& \quad \gamma^2 \int_{\mathbb{R}^d} dv_2 \int_{\mathbb{R}^d} dv_3 \left(\|v_3\|^2 + \|v_1\|^2 \right) \left(\|v_3\|^2 + \|v_2\|^2 \right) M(\sigma, v_2) M(\sigma, v_3) \\
& = \kappa^2 + \kappa \gamma \left(3 d \sigma^2 + \|v_1\|^2 \right) + \gamma^2 \left(2 d (d + 1) \sigma^4 + 2 d \sigma^2 \|v_1\|^2 \right),
\end{aligned}$$

the one-particle marginal is

$$\begin{aligned}
f_{3,1}(t, v) &= \frac{2}{3I(t, 3)} M(\sigma_\gamma(t), v) \times \\
& \quad \left[\gamma^2 \|v\|^4 + \left(4 \kappa \gamma + 6 d \gamma^2 \sigma_\gamma^2(t) \right) \|v\|^2 + 3 \kappa^2 + 8 d \kappa \gamma \sigma_\gamma^2(t) + d (5 d + 4) \gamma^2 \sigma_\gamma^4(t) \right].
\end{aligned} \tag{4.58}$$

For simplicity, we assume $\kappa = 0$. According to (4.57) and (4.58), the **one-particle energy** (4.19) takes the form (cf. (4.13))

$$\begin{aligned}
E_3(t) &= \frac{\gamma^2 d (d + 2) (d + 4) \sigma_\gamma^6(t) + 6 \gamma^2 d^2 (d + 2) \sigma_\gamma^6(t) + \gamma^2 d^2 (5 d + 4) \sigma_\gamma^6(t)}{6 d (2 d + 1) \gamma^2 \sigma_\gamma^4(t)} \\
&= \frac{d^2 + 6 d + 8 + 6 d^2 + 12 d + 5 d^2 + 4 d}{6 (2 d + 1)} \sigma_\gamma^2(t) \\
&= \frac{6 d^2 + 11 d + 4}{3 (2 d + 1)} \sigma_\gamma^2(t) = \frac{3 d + 4}{3} \sigma_\gamma^2(t).
\end{aligned} \tag{4.59}$$

Note that

$$\begin{aligned}
& \int_{\mathbb{R}^d} \int_{\mathbb{R}^d} (v_1, v_2)^2 \|v_1\|^2 M(\sigma, v_1) M(\sigma, v_2) dv_1 dv_2 = \\
& \quad d \int_{\mathbb{R}^d} \int_{\mathbb{R}^d} \left(v_{1,1}^2 v_{2,1}^2 + \dots + v_{1,d}^2 v_{2,d}^2 \right) v_{1,1}^2 M(\sigma, v_1) M(\sigma, v_2) dv_1 dv_2 \\
& = d (3 \sigma^4 \sigma^2 + (d - 1) \sigma^6) = d (d + 2) \sigma^6
\end{aligned} \tag{4.60}$$

and

$$\begin{aligned} \int_{\mathbb{R}^d} \int_{\mathbb{R}^d} \int_{\mathbb{R}^d} (v_1, v_2) (v_1, v_3) (v_3, v_2) \left[\prod_{i=1}^3 M(\sigma, v_i) \right] dv_1 dv_2 dv_3 &= \quad (4.61) \\ d \int_{\mathbb{R}^d} \int_{\mathbb{R}^d} \int_{\mathbb{R}^d} v_{1,1}^2 v_{2,1}^2 v_{3,1}^2 \left[\prod_{i=1}^3 M(\sigma, v_i) \right] dv_1 dv_2 dv_3 &= d \sigma^6. \end{aligned}$$

According to (4.48), (4.60) and (4.61), one obtains

$$\begin{aligned} \int_{\mathbb{R}^d} \int_{\mathbb{R}^d} \int_{\mathbb{R}^d} (v_1, v_2) \|v_1 - v_2\|^2 \|v_1 - v_3\|^2 \left[\prod_{i=1}^3 M(\sigma, v_i) \right] dv_1 dv_2 dv_3 &= \\ \int_{\mathbb{R}^d} \int_{\mathbb{R}^d} \int_{\mathbb{R}^d} (v_1, v_2) \|v_2 - v_3\|^2 \|v_2 - v_1\|^2 \left[\prod_{i=1}^3 M(\sigma, v_i) \right] dv_1 dv_2 dv_3 &= \\ = -2 \int_{\mathbb{R}^d} \int_{\mathbb{R}^d} \int_{\mathbb{R}^d} (v_1, v_2)^2 \left(\|v_1\|^2 + \|v_3\|^2 \right) \left[\prod_{i=1}^3 M(\sigma, v_i) \right] dv_1 dv_2 dv_3 &= \\ = -2 \left[d(d+2) \sigma^6 + d \sigma^4 d \sigma^2 \right] = -4 d(d+1) \sigma^6 & \quad (4.62) \end{aligned}$$

and

$$\begin{aligned} \int_{\mathbb{R}^d} \int_{\mathbb{R}^d} \int_{\mathbb{R}^d} (v_1, v_2) \|v_3 - v_1\|^2 \|v_3 - v_2\|^2 \left[\prod_{i=1}^3 M(\sigma, v_i) \right] dv_1 dv_2 dv_3 &= \quad (4.63) \\ 4 \int_{\mathbb{R}^d} \int_{\mathbb{R}^d} \int_{\mathbb{R}^d} (v_1, v_2) (v_1, v_3) (v_2, v_3) \left[\prod_{i=1}^3 M(\sigma, v_i) \right] dv_1 dv_2 dv_3 &= 4 d \sigma^6. \end{aligned}$$

It follows from (4.55), (4.56), (4.57), (4.62) and (4.63) that

$$\begin{aligned} \int_{\mathbb{R}^d} \int_{\mathbb{R}^d} (v_1, v_2) f_{3,2}(t, v_1, v_2) dv_1 dv_2 &= \quad (4.64) \\ \frac{\gamma^2}{6 d (2 d + 1) \gamma^2 \sigma_\gamma^4(t)} \left[-8 d (d + 1) \sigma_\gamma^6(t) + 4 d \sigma_\gamma^6(t) \right] &= \\ = \frac{1}{6 d (2 d + 1)} \left[-8 d (d + 1) + 4 d \right] \sigma_\gamma^2(t) = -\frac{2}{3} \sigma_\gamma^2(t). & \end{aligned}$$

According to (4.59) and (4.64), the **two-particle correlation coefficient** (4.20) takes the form

$$r_3(t) = -\frac{2}{3d+4}. \quad (4.65)$$

4.3 Numerical experiments

We study properties of the stochastic model with the binary interaction rates (4.28) (hard sphere case) and (4.35), where $\kappa = 0$ and $\gamma = \gamma^{\text{Qu}} > 0$ (quadratic case). These rates are of the form

$$B_1(v, w) = \gamma \|v - w\|^k, \quad v, w \in \mathbb{R}^d, \quad (4.66)$$

where $\gamma > 0$ and $k \in \mathbb{R}$ are parameters. Using terms from kinetic theory, the values $k \in (0, 1)$ correspond to “hard potentials”, while the values $k < 0$ correspond to “soft potentials” and $k = 0$ corresponds to “Maxwell molecules” (constant case). We also consider the rate function

$$B_1(v, w) = \gamma 1_{\|v-w\| \leq \varepsilon}, \quad v, w \in \mathbb{R}^d, \quad (4.67)$$

where $\gamma, \varepsilon > 0$ are parameters. This “step function case” is similar to (4.66) with $k < 0$ in the sense that pairs of particles with small relative velocities are preferentially chosen to interact. However, the function (4.67) is easier to implement in the numerical algorithm.

There are three main goals of the numerical experiments:

- Check the analytical formulas in the quadratic case.
- Illustrate that the hard sphere case is qualitatively similar to the quadratic case.
- Find properties that are qualitatively different in the step function case.

When comparing the quadratic and the hard sphere case, the parameters are chosen in such a way that the mean free times are the same. According to (3.55) and (4.15), one obtains

$$t_{\text{mf}} = \frac{\Gamma(\frac{d}{2})}{\gamma \sigma^k 2^{k+1} \Gamma(\frac{d+k}{2})}, \quad k > -d,$$

so that

$$t_{\text{mf}}^{\text{HS}} = t_{\text{mf}}^{\text{Qu}} = 1 \quad (4.68)$$

if

$$\gamma^{\text{HS}} = \frac{\Gamma(\frac{d}{2})}{4 \sigma \Gamma(\frac{d+1}{2})} \quad \text{and} \quad \gamma^{\text{Qu}} = \frac{1}{4 \sigma^2 d}. \quad (4.69)$$

When considering the step function case (4.67), the parameters are chosen so that the mean free time equals (4.68). The number of particles is $n = 2^{20}$. The parameter of the initial state (4.9) is $\sigma = 1$. Independent repetitions are used in order to reduce the statistical fluctuations and to construct confidence intervals. The number of repetitions is $N_{\text{rep}} = 10$.

4.3.1 Cluster properties

Here we study the functionals (4.19) and (4.20) in order to illustrate properties of the cluster distributions. We consider $d = 3$ and use $\varepsilon = 1$ in the step function case (4.67).

One-particle energies

According to (4.41), (4.45), (4.51), (4.59) and (4.69), one obtains in the quadratic case

$$E_x(t) = \frac{e(x) \sigma^2}{1 + 4 t \gamma^{\text{Qu}} \sigma^2} = \frac{e(x) \sigma^2}{1 + t/d}, \quad x = 1, 2, 3, \quad (4.70)$$

where

$$e(1) = d, \quad e(2) = d + 1, \quad e(3) = \frac{6d^2 + 11d + 4}{3(2d + 1)}$$

so that, for $d = 3$,

$$e(1) = 3, \quad e(2) = 4, \quad e(3) = 4.33. \quad (4.71)$$

In the constant case one obtains (cf. (4.11), (4.39))

$$E_x(t) = d\sigma^2, \quad x = 1, 2, \dots$$

Note that the property $E_1(0) = d\sigma^2$ holds in all cases.

- Figure 1 shows the quantity $E_1(t)$ in all three cases.

In the quadratic case the numerical results are compared with the prediction $E_1(t) = \frac{9}{3+t}$. In the hard sphere case the singleton energy also decreases with time, but slower than in the quadratic case.

In the step function case the singleton energy increases. This can be explained by properties of the rate function and the initial distribution. Pairs of particles with small relative velocities are preferentially chosen to interact. Due to the form of the Maxwellian there are more such pairs around the origin.

- Figure 2 shows the quantities $\frac{E_x(t)}{E_1(t)}$, for $x = 2, 3$, in all three cases.

In the quadratic case the numerical results are compared with the predictions 1.33 (for $x = 2$) and 1.44 (for $x = 3$) based on (4.70), (4.71). In the hard sphere case the quantities are almost constant with respect to t (cf. Figure 3) and also increase with respect to x .

In the step function case the one-particle energies are not constant with respect to t . Moreover, they decrease with respect to x .

- Figure 3 shows the quantities $\frac{E_x(t)}{E_1(t)}$, for $x = 2, 3, 4$, in the hard sphere case.

It contains a zoom of Figure 2. The quantities are not constant with respect to t and increase with respect to x .

Two-particle correlations

According to (4.51), (4.65), one obtains in the quadratic case

$$r_2(t) = -\frac{1}{d+1}, \quad r_3(t) = -\frac{2(d+4)}{6d^2 + 11d + 4}$$

so that, for $d = 3$,

$$r_2(t) = -0.25, \quad r_3(t) = -\frac{2}{13} = -0.154. \quad (4.72)$$

In the constant case one obtains $r_x(t) = 0$, $x = 2, 3, \dots$ (cf. (4.39)).

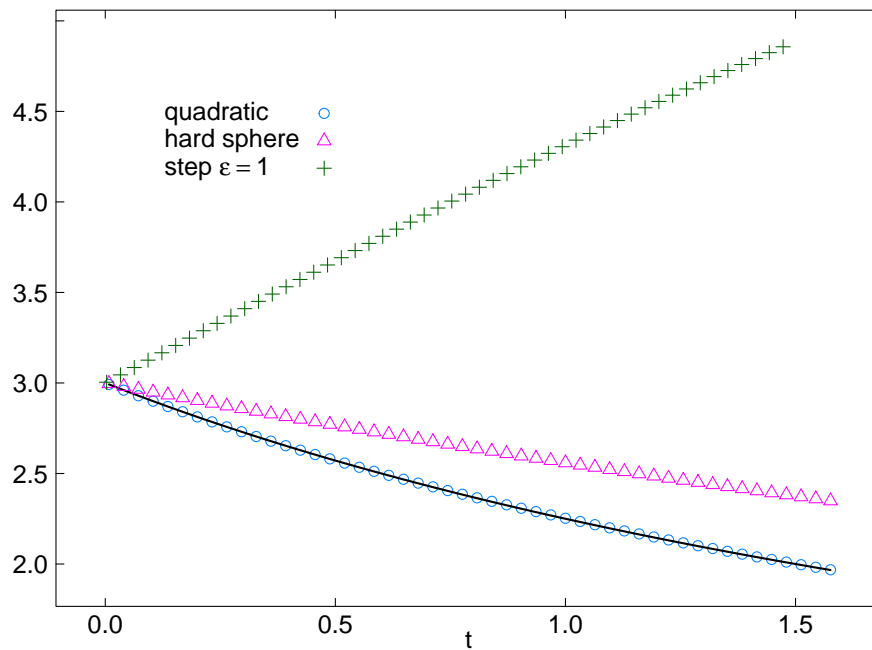


Figure 1: Quantity $E_1(t)$ in the quadratic, hard sphere and step function cases. The solid line shows the prediction in the quadratic case.

- Figure 4 shows the quantities $r_x(t)$, for $x = 2, 3$, in all three cases.

In the quadratic case the numerical results are compared with the predictions (4.72). In the hard sphere case the two-particle correlation coefficients are also negative, almost constant with respect to t , and increasing with respect to x .

In the step function case the two-particle correlation coefficients are positive and not constant with respect to t . Moreover, they decrease with respect to x .

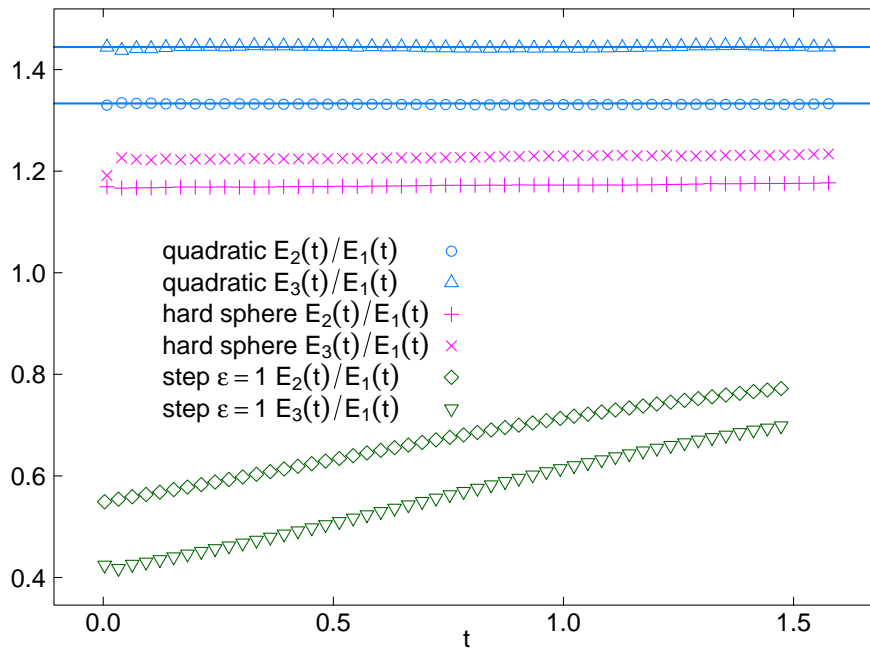


Figure 2: Quantities $\frac{E_x(t)}{E_1(t)}$, for $x = 2, 3$, in the quadratic, hard sphere and step function cases. The solid lines show the predictions in the quadratic case.

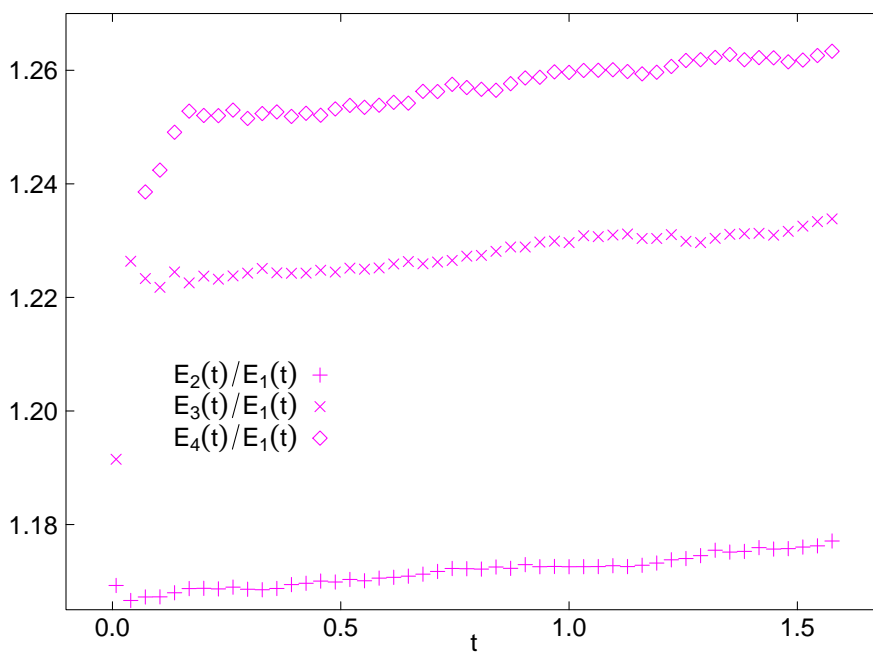


Figure 3: Quantities $\frac{E_x(t)}{E_1(t)}$ in the hard sphere case for $x = 2, 3, 4$.

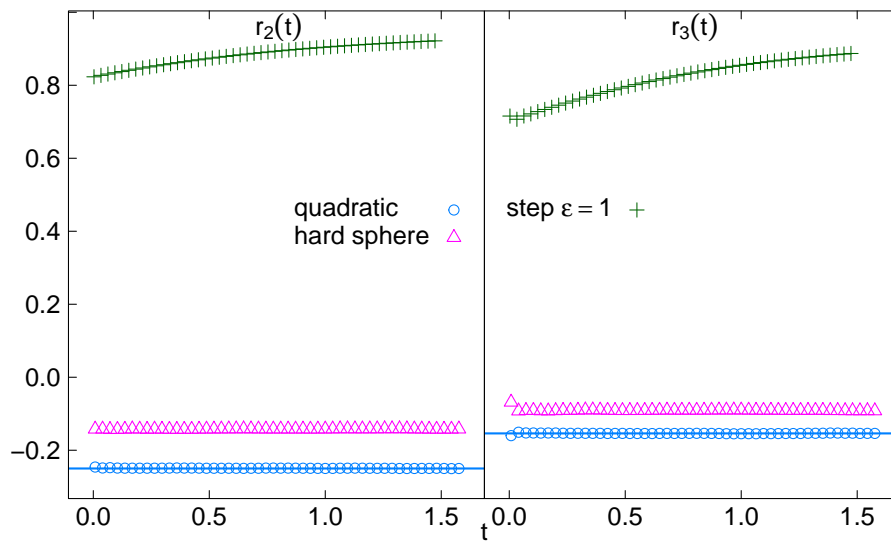


Figure 4: Quantities $r_x(t)$ in the quadratic, hard sphere and step function cases, for $x = 2$ (left) and $x = 3$ (right). The solid lines show the predictions in the quadratic case.

4.3.2 Gelation time

Here we study properties of the gelation time (3.48). The first two figures are obtained in the hard sphere case with $d = 3$. They reproduce the corresponding results obtained with the billiard model (see [6, Figs.1,2] and [11, Figs.1,2]). The results in the quadratic case and in the step function case are qualitatively the same.

- Figure 5 shows the sizes (in logarithmic scale) of all clusters for a single realization of the system. This figure illustrates the phase transition.
- Figure 6 shows the cluster size distribution $c(t, x)$ (in a log-log scale) before, at and after the gelation time. This distribution is compared with the power law with exponent $-\frac{5}{2}$. For small concentrations, the accuracy is limited by the finite number of particles.

Next we perform quantitative measurements of the gelation time. We measure the second moment (cf. (3.30)) for the system without the largest component. The time, where this function takes its maximum, is used as an approximation for the gelation time. If the rate function has the form (4.66), then one obtains (cf. (4.21), (4.22))

$$t_{\text{mf}}(\gamma, \sigma) = \frac{1}{\gamma \sigma^k} t_{\text{mf}}(1, 1) \quad \text{and} \quad t_{\text{gel}}(\gamma, \sigma) = \frac{1}{\gamma \sigma^k} t_{\text{gel}}(1, 1)$$

so that

$$\frac{t_{\text{gel}}(\gamma, \sigma)}{t_{\text{mf}}(\gamma, \sigma)} = \frac{t_{\text{gel}}(1, 1)}{t_{\text{mf}}(1, 1)}.$$

Due to these scaling properties, the measurements provide the same results for any parameters γ and σ . In the step function case (4.67) the scaling with respect to γ is the same. However, the scaling with respect to σ depends on ε . Namely, the parameters σ, ε correspond to $1, \frac{\varepsilon}{\sigma}$. Therefore, the measurements are performed for different ε .

- Figure 7 shows the dependence of the quantity $\frac{t_{\text{gel}}}{t_{\text{mf}}}$ on the dimension in the hard sphere case. For $d = 3$, one obtains a value

$$\frac{t_{\text{gel}}}{t_{\text{mf}}} \sim 0.97. \quad (4.73)$$

In the quadratic case, with $d = 3$, one obtains

$$\frac{t_{\text{gel}}}{t_{\text{mf}}} \sim 0.89 \pm 0.01.$$

- Figure 8 shows the dependence of the quantity $\frac{t_{\text{gel}}}{t_{\text{mf}}}$ on the step length ε in the step function case (4.67), where $d = 3$. The quantity is increasing with ε . For $\varepsilon \rightarrow \infty$, one obtains $B_1 \rightarrow \gamma$ so that $\frac{t_{\text{gel}}}{t_{\text{mf}}} \rightarrow 1$. A linear fit of the values for $\varepsilon \leq 1$ is $0.26 \varepsilon + 0.36$.

Figures 7 and 8 suggest the **conjecture**

$$t_{\text{gel}} \leq t_{\text{mf}}. \quad (4.74)$$

In the constant case (cf. (3.78)) there is equality in (4.74). The conjecture is expected to hold for rather general (if not arbitrary) interaction kernels. It is fulfilled, e.g., for the example with multi-colour clusters (cf. (3.99)).

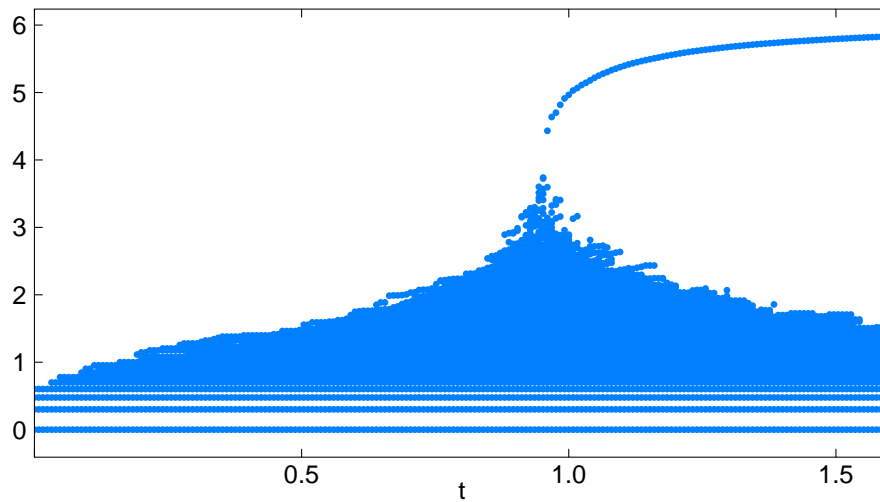


Figure 5: Sizes of all clusters for a single realization of the system (logarithmic scale).

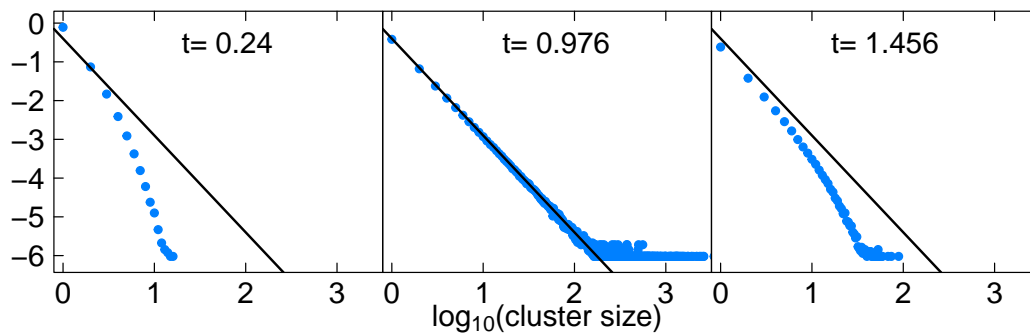


Figure 6: Cluster size distribution before, at and after the gelation time (log-log scale). The solid lines show the power law with exponent $-\frac{5}{2}$.

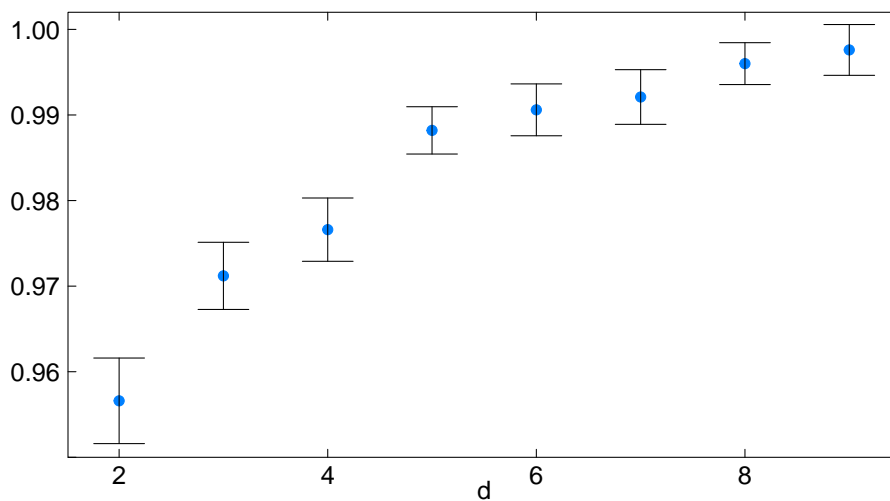


Figure 7: Quantity $\frac{t_{gel}}{t_{mf}}$ versus dimension in the hard sphere case, with 95%-confidence intervals.

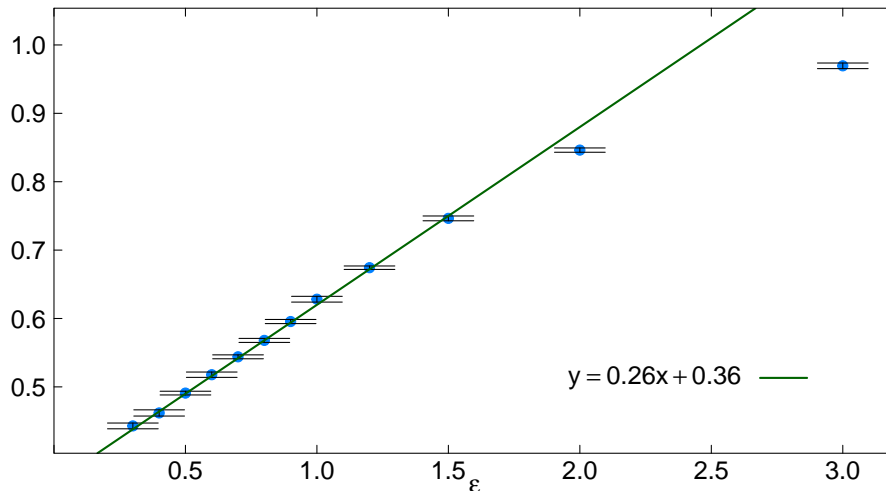


Figure 8: Quantity $\frac{t_{\text{gel}}}{t_{\text{mf}}}$ versus step length in the step function case, with 95%-confidence intervals ($N_{\text{rep}} = 25$).

4.3.3 Billiard model

Here we discuss the relationship between our numerical observations (for the stochastic model) and numerical results from [6] and [11] (for the billiard model). Qualitatively all results are consistent (cf. Figure 5 concerning the existence of a critical time and Figure 6 concerning the behaviour of the cluster size distribution). However, quantitatively the numerical results from both papers on the billiard model partly contradict our observations. Moreover, these results are partly not consistent with each other. In Remarks 4.1 and 4.2 we will provide some speculations about how these inconsistencies could be explained and removed.

Results from [6]

Consider $d = 2$ and the parameter (“density”, better “volume fraction”, cf. (4.25))

$$\varrho = \frac{N \pi r^2}{V}, \quad (4.75)$$

where V is the area of a square of side length L . The parameter of the initial Maxwellian (4.9) is $\sigma = 1$. The critical time is defined as

$$t_c = \inf\{t > 0 : M_1(t) > M_2(s), \forall s > t\}, \quad (4.76)$$

where $M_i(t)$ denotes the size of the i -th largest cluster at time t . The model is run until the instant when a cluster of mass $0.95 N$ is formed. In particular, the following results are obtained:

- Figure 4 (from [6]) shows t_c dependent on ϱ , where $N = 5 \times 10^3$. The numerical observations are summarized in the formula

$$t_c \sim 0.4 \varrho^{-1}. \quad (4.77)$$

- Figure 6 (from [6]) shows $\frac{M_1(t)}{N}$ dependent on t and N , where $10 \leq N \leq 10^4$ and $\varrho = 10^{-3}$. The results indicate a value close to 400 for t_c , which is consistent with (4.77).

According to (4.32) and (4.75), one obtains $r = \sqrt{(V \varrho)/(\pi N)}$ and

$$t_{\text{mf}}^{\text{HS}} = \frac{1}{4} \sqrt{\frac{V}{N \varrho}}. \quad (4.78)$$

However, the prediction $t_{\text{gel}} \sim 0.96 \times t_{\text{mf}}^{\text{HS}}$ (cf. Figure 7 and (4.78)) contradicts both (4.77) and the stability with respect to N observed in Figure 6 (from [6]).

Remark 4.1 *When choosing the parameter*

$$\varrho = \alpha N r^{d-1}, \quad \text{for some } \alpha > 0,$$

which stays constant in the Boltzmann-Grad limit, then (4.32) implies

$$t_{\text{mf}}^{\text{HS}} = \frac{\alpha V \Gamma(\frac{d}{2})}{2^d \pi^{\frac{d-1}{2}}} \varrho^{-1}. \quad (4.79)$$

In particular, when replacing (4.75) by

$$\varrho = \frac{N \pi r}{V},$$

then (4.79) takes the form

$$t_{\text{mf}}^{\text{HS}} = \frac{\sqrt{\pi}}{4} \varrho^{-1} \sim 0.44 \varrho^{-1},$$

which is consistent with (4.77).

Results from [11]

Consider the domain $(0, 1)^d$ and the parameter (cf. (4.31))

$$\varrho = |D_d(r)| N = \frac{r^d \pi^{\frac{d}{2}} N}{\Gamma(\frac{d}{2} + 1)}. \quad (4.80)$$

The total mass of the system is assumed to be 1 so that the parameter of the initial Maxwellian (4.9) is

$$\sigma^2 = \frac{1}{m} = N. \quad (4.81)$$

The definitions of the critical time and the run time are the same as in [6] (cf. (4.76)). In particular, the following results are obtained:

d	ϱ	N	t_c	t_{mf}
2	0.1	1000	1.27	0.79
2	0.01	1000	3.16	2.5
2	0.001	1000	7.81	7.9
2	0.01	2500	3.26	2.5
4	0.1	1000	0.71	1.2
4	0.01	1000	5.68	6.6
4	0.001	1000	32.2	37
4	0.01	2500	7.58	8.3
6	0.01	2500	2.00	4.4
6	0.01	1000	1.33	3.3
6	0.001	1000	11.7	22

Table 1: This is Table 1 from [11] extended by results for t_{mf} obtained according to (4.85).

- Figure 3 (from [11]) shows t_c dependent on d , where $\varrho = 10^{-1}, 10^{-2}, 10^{-3}, 10^{-4}$ and $N = 10^3$.
- Figure 4 (from [11]) shows t_c dependent on the average time between collisions $\langle \tau_d \rangle$. The numerical observations (for $N = 10^3$) are summarized in the formulas

$$t_c = 0.6 + 471 \langle \tau_2 \rangle, \quad t_c = 0.2 + 485 \langle \tau_4 \rangle, \quad t_c = 0.2 + 454 \langle \tau_6 \rangle. \quad (4.82)$$

Since $\langle \tau_d \rangle$ refers to the whole system, one obtains $t_{mf}(d) = \langle \tau_d \rangle \times \frac{N}{2}$ so that (4.82) implies

$$\begin{aligned} t_c(2) &= 0.6 + 0.94 t_{mf}(2), & t_c(4) &= 0.2 + 0.97 t_{mf}(4), \\ t_c(6) &= 0.2 + 0.91 t_{mf}(6). \end{aligned} \quad (4.83)$$

Formulas (4.83) are consistent with our numerical measurements (cf. Figure 7).

According to (4.32), (4.80) and (4.81), one obtains $r^{d-1} = [\varrho \Gamma(\frac{d}{2} + 1)]^{\frac{d-1}{d}} / (\pi^{\frac{d-1}{2}} N^{\frac{d-1}{d}})$ and

$$t_{mf}^{HS} = \left[\frac{[\varrho \Gamma(\frac{d}{2} + 1)]^{\frac{d-1}{d}}}{\pi^{\frac{d-1}{2}} N^{\frac{d-1}{d}}} N \sigma \frac{2^d \pi^{\frac{d-1}{2}}}{\Gamma(\frac{d}{2})} \right]^{-1} = G(d) \frac{1}{\varrho^{1-\frac{1}{d}}} \frac{1}{N^{\frac{1}{2}+\frac{1}{d}}}, \quad (4.84)$$

where

$$G(d) = \frac{\Gamma(\frac{d}{2} + 1)^{\frac{1}{d}}}{2^{d-1} d}.$$

Some numerical values from Figure 3 (from [11]) are displayed in Table 1. Note that the values for $d = 2$ are not in agreement with the results from [6]. In particular, the dependence of the critical time t_c on ϱ it is not like ϱ^{-1} as in (4.77), but close to $\varrho^{-1/2}$ as predicted by (4.84). However, the quantitative predictions of the critical time based on (4.84) are not consistent with the observed values in Table 1. Both quantities differ by several orders of magnitude. The dependence on N is even qualitatively wrong in the sense that the quantities (4.84) decrease with N , while the values in Table 1 increase with N .

Remark 4.2 When replacing (4.81) by $\sigma^2 = N^{-1}$, then (4.84) takes the form

$$t_{\text{mf}}^{\text{HS}} = G(d) \frac{1}{\varrho^{1-\frac{1}{d}}} N^{\frac{1}{2}-\frac{1}{d}}. \quad (4.85)$$

The corresponding values are displayed in the last column of Table 1. The predictions based on (4.85) are consistent with the observed values. In particular, the dependence on N is recovered quite well.

5 Comments

We have considered a stochastic particle model with a general binary interaction kernel. A kinetic equation for the distribution of interaction clusters was found. Moreover, a phase transition in the cluster formation process was established in analogy with [6], where the frictionless elastic billiard model was studied. The generality of our model provides a better understanding of the basic mechanism of the phase transition. In particular, the model also covers rarefied gases with inelastic collisions. The kinetic equation generalizes Smoluchowski's coagulation equation with the multiplicative kernel (cf. (3.79), (3.80)). This kernel has its origin in polymer physics, from where the term “gelation” also comes. We refer to the introduction of [21] for more details. Our model extends this connection to polymers with an internal structure. Similar objects are used in certain advanced models of soot formation, which are of interest in chemical engineering (see, e.g., [9]).

The classical polymer model (multiplicative coagulation kernel) has a close connection with random graph theory. Our model can be interpreted in terms of “random graphs in random environment”. Indeed, consider n vertices, each having a random state (label, colour) v_i , $i = 1, \dots, n$. Edges are created with rates $B_1(v_i, v_j)$. The interaction clusters correspond to random partitions of the index set. Various special cases can be interpreted in terms of the environment. In the general case there is a “dynamic environment”, which can be stationary or non-stationary. In Example 3.6 there is a “static environment”. In the case of constant B_1 there is a “deterministic environment”, which corresponds to the standard random graph model. It is interesting to consider the model with the “averaged environment”. In this case the rates for choosing the edges are constant,

$$B_1^{\text{aver}} \sim \int_{\mathbb{V}^2} B_1(v, w) \pi(dv) \pi(dw).$$

According to (3.55) and (3.78), one obtains

$$t_{\text{gel}}^{\text{aver}} = t_{\text{mf}}$$

so that (4.74) implies

$$t_{\text{gel}} \leq t_{\text{gel}}^{\text{aver}}.$$

Thus, the phase transition in the model with the random environment happens earlier than in the model with the averaged environment.

The case of Boltzmann type interactions (leading to the Boltzmann equation) is covered by our model. For a special (quadratic) collision kernel some analytic formulas for the cluster distribution were obtained. These formulas were checked by numerical experiments, which provides a certain empirical validation. We believe that the cluster distribution for the original billiard model is asymptotically (in the Boltzmann-Grad limit) the same as for the stochastic model with the corresponding hard sphere kernel. In view of Remarks 4.1 and 4.2, it would be of interest to repeat (some of) the numerical experiments with the billiard model. The explicit tree representation for the cluster size distribution obtained in [15] starting from the deterministic collision model can be derived from the kinetic equation for the cluster distribution obtained from the stochastic model.

So far there is no rigorous proof of the transition from the finite particle system to the limiting kinetic equation for the cluster distribution. There are only predictions based on heuristic derivations, which are supported by numerical experiments. The proof for the billiard model would be extremely challenging, since it includes the corresponding proof for the Boltzmann equation as a pre-requisite. On the other hand, it seems to be feasible to extend the proof technique from [14] to our stochastic model (cf. Remark 3.1). However, the above remarks about the “random environment” indicate that the convergence issue is not trivial at all. In connection with the rigorous justification for the stochastic model, it might be possible to study also the spatially inhomogeneous situation and the post-gelation behaviour. A stochastic particle model for the spatially inhomogeneous (mollified) Boltzmann equation goes back to [10]. We refer to [17, Section 2.3.3] and [22] for more details and references concerning this issue. In this case the random environment is a piecewise-deterministic Markov process. Some results concerning the post-gelation behaviour can be found in [14, 18, 21]. Finally, an important open problem for the general stochastic model is to find either a theoretical justification or a counter-example for the conjecture that the gelation time does not exceed the mean free time.

References

- [1] G. A. BIRD, *Molecular Gas Dynamics and the Direct Simulation of Gas Flows*, vol. 42 of Oxford Engineering Science Series, Clarendon Press, Oxford, 1994.
- [2] C. CERCIGNANI, *The Boltzmann Equation and its Applications*, Springer, New York, 1988.
- [3] C. CERCIGNANI, R. ILLNER, AND M. PULVIRENTI, *The Mathematical Theory of Dilute Gases*, Springer, New York, 1994.
- [4] A. EIBECK AND W. WAGNER, *Stochastic interacting particle systems and nonlinear kinetic equations*, Ann. Appl. Probab., 13 (2003), pp. 845–889.
- [5] A. GABRIELOV, V. KEILIS-BOROK, S. OLSEN, AND I. ZALIAPIN, *Predictability of extreme events in a branching diffusion model*, in Extreme natural hazards, disaster risks and societal implications, Cambridge University Press, 2014, pp. 126–142.
- [6] A. GABRIELOV, V. KEILIS-BOROK, Y. SINAI, AND I. ZALIAPIN, *Statistical properties of the cluster dynamics of the systems of statistical mechanics*, in Boltzmann’s legacy, ESI Lect. Math. Phys., Eur. Math. Soc., Zürich, 2008, pp. 203–215.

- [7] I. GALLAGHER, L. SAINT-RAYMOND, AND B. TEXIER, *From Newton to Boltzmann: hard spheres and short-range potentials*, Zurich Lect. in Adv. Mathematics, Eur. Math. Soc., Zürich, 2013.
- [8] M. KAC, *Foundations of kinetic theory*, in Third Berkeley Symposium on Mathematical Statistics and Probability Theory, vol. 3, Berkeley and Los Angeles, 1956, University of California Press, pp. 171–197.
- [9] K. F. LEE, R. I. A. PATTERSON, W. WAGNER, AND M. KRAFT, *Stochastic weighted particle methods for population balance equations with coagulation, fragmentation and spatial inhomogeneity*, J. Comput. Phys., 303 (2015), pp. 1–18.
- [10] M. A. LEONTOVICH, *Basic equations of the kinetic theory of gases from the point of view of the theory of random processes*, Zhurnal Eksper. Teoret. Fiziki, 5 (1935), pp. 211–231. In Russian.
- [11] C. MCFADDEN AND L.-S. BOUCHARD, *Universality of cluster dynamics*, Phys. Rev. E, 82 (2010), p. 061125.
- [12] J. B. MCLEOD, *On an infinite set of non-linear differential equations*, Quart. J. Math. Oxford Ser. (2), 13 (1962), pp. 119–128.
- [13] S. MISCHLER AND C. MOUHOT, *Kac’s program in kinetic theory*, Inventiones mathematicae, 193 (2013), pp. 1–147.
- [14] J. R. NORRIS, *Cluster coagulation*, Comm. Math. Phys., 209 (2000), pp. 407–435.
- [15] R. I. A. PATTERSON, S. SIMONELLA, AND W. WAGNER, *Kinetic theory of cluster dynamics*, Physica D: Nonlinear Phenomena, 335 (2016), pp. 26–32.
- [16] M. PULVIRENTI AND S. SIMONELLA, *The Boltzmann-Grad limit of a hard sphere system: analysis of the correlation error*, Inventiones mathematicae, (2016), pp. 1–103.
- [17] S. RJASANOW AND W. WAGNER, *Stochastic Numerics for the Boltzmann Equation*, Springer, Berlin, 2005.
- [18] R. SIEGMUND-SCHULTZE AND W. WAGNER, *Induced gelation in a two-site spatial coagulation model*, Ann. Appl. Probab., 16 (2006), pp. 370–402.
- [19] H. SPOHN, *Large Scale Dynamics of Interacting Particles*, Springer, Heidelberg, 1991.
- [20] W. WAGNER, *A convergence proof for Bird’s direct simulation Monte Carlo method for the Boltzmann equation*, J. Statist. Phys., 66 (1992), pp. 1011–1044.
- [21] ———, *Post-gelation behavior of a spatial coagulation model*, Electron. J. Probab., 11 (2006), pp. 893–933.
- [22] ———, *Stochastic models in kinetic theory*, Phys. Fluids, 23 (2011), pp. 030602(1–14).